7-2016

THE EXPERIMENT AND ANALYSIS OF ACTIVE MECHANISMS FOR ENHANCING HEAT AND MASS TRANSFER IN SORPTION FLUIDS

ziqi shen
University of Nebraska-Lincoln, zshen@unomaha.edu

THE EXPERIMENT AND ANALYSIS OF ACTIVE MECHANISMS FOR ENHANCING HEAT AND MASS TRANSFER IN SORPTION FLUIDS

by

Ziqi Shen

A THESIS

Presented to the Faculty of

The Graduate College at the University of Nebraska

In Partial Fulfillment of Requirements

For the Degree of Master of Science

Major: Architectural Engineering

Under the Supervision of Professor Yuebin Yu

Lincoln, Nebraska

July, 2016

THE EXPERIMENT AND ANALYSIS OF ACTIVE MECHANISMS FOR ENHANCING HEAT AND MASS TRANSFER IN SORPTION FLUIDS

Ziqi Shen, M.S.

University of Nebraska, 2016

Advisor: Yuebin Yu

This project was funded by American Society of Heating, Refrigerating, and Air-Conditioning Engineers (ASHRAE RP-1462). It is a three years' research, including the literature review, labs construction, experiments and data analysis.

In this thesis, first of all, we conducted literature review of mechanism motion influence on heat and mass transfer and additive effect in absorption chiller. This part helps us understand the basic idea of how mechanism motion affects the heat and mass transfer of sorption fluids and gives us reference on how to select the experiment instrument and the experiment operation range.

In the second part, the instrument selection and lab construction are introduced. A commercial absorption chiller, a vertical vibration table and a statistic water loop system are used in our lab. This test facility has the capability of realizing mechanism motion in real systems with adjustable wide range vibration and long term stabilized auxiliary water supply. A commercial absorption chiller with a

capacity of 10kW is utilized in this project. A water loop system was constructed to maintain a repetitive experimental condition when the outdoor conditions change. We also installed a data acquisition system for in-line measurement of the solution concentration and temperature and flow rate of the solution and water loops. We can use these measurements to calculate the heat and mass transfer capacity in the absorber in steady-state. The enhancement is obtained by comparing the temperature differences, before a vibration and during a vibration.

In the third section, we illustrate the methodology of how to analyze the heat and mass transfer in the absorber and the data under different conditions. We separate the experiment into three big groups, including the conditions without additive, with n-octanol additive and with 2-ethylhexanol(2EH) additive. Different film thickness (spray amount), vibration frequency, and vibration amplitude comparisons were considered under each condition. And we also cross-compared all these three groups. The results of this project revealed the optimal frequency and amplitude combinations (at 25 Hz & 0.2mm) for the absorption chiller tested in this study. The results of this project provided information filling the knowledge gap about the influence of mechanical motion in absorption chiller technology.

ACKNOWLEDGEMENTS

I would like to express my deepest gratitude to my advisor Dr. Yuebin Yu. He is very patient and gave me huge help in my last few years' research and study. He pointed out my shortage and help me improve my time management, writing habits and a lot of things I am lack of. And he is also a professor with an open mind. He encouraged and helped me improve my ideas and systematic analysis of anything new. He always gave me useful and great advices on how to improve this research. His encouragement and persistence have inspired me to become consistent, reliable, and hard-working, traits that I believe will continue to help me throughout my entire life.

My gratitude also goes to Dr. Josephine Lau. She is one of the most important members in this research. She led me into the research area and taught me how to seriously treat research and study. This will help not only in my study, but also in my further work.

I would like to thank Dr. Zhang Tian and Dr. Moe. You gave me precious comments and advices. I also want to thank the engineers who build the lab for our experiment. Shuangliang Energy Cooperation, Dongling LTD and Dingtuo INC. I would like to thank Tianjin University of Commerce who provides huge help to this project.

Finally, I want to thank my dad for the support. Without him, the experiment could not be conducted such smoothly. He used almost all of his resource to help our group build the lab and finish the experiments. And I want to thank my mom; she is always supportive to me. And thank you all the friends who helped and encouraged me in the past few years.

TABLE OF CONTENTS

Chapter 1 Introduction

1.1 Introduction

Today social and economic development is facing the threat of primary energy being increasingly exhausted. A lithium bromide absorption chiller is an effective refrigeration system that can use low-grade thermal energy for cooling. However, the refrigeration efficiency of an absorption chiller is not high compared to a mechanical vapor compression cycle. Heat and mass transfer reinforcement for a lithium bromide absorption chiller has been the main direction of research.

Producing cooling effect from absorption refrigeration systems can be traced back to almost a century ago. In their emerging stage, however, with relatively low coefficient of performance (COP), they could not keep pace with the popularity of vapor compression systems that were commercialized later. In recent years, with ever-growing prices of energy from one hand, and the existing battle against greenhouse gases (GHG) emissions from the other, absorption refrigeration systems caught the attention of researchers and industries. They are becoming commercially more accessible for various applications and climatic conditions through the introduction of modified and adapted machines.

Similar to the physical processes in a conventional vapor compression cycle, the absorption system uses its thermal compressor (including a generator, absorber, pump and heat exchangers) to vaporize the water out of a lithium bromide/water solution and compress the water vapor to a higher pressure. The cycle is illustrated in Fig. 1-1. The

compressed hot refrigerant vapor then condenses to the liquid state in a condenser. Heat is rejected from the high-pressure refrigerant water inside the condenser into the cooling water flowing through the condenser. The high-pressure liquid water then passes through a throttling valve to reduce its pressure. Then, the low-pressure liquid water enters the evaporator and evaporates from the liquid phase to the vapor phase; heat is absorbed from the chilled water into the refrigerant vapor in the vaporization process. Vapor is

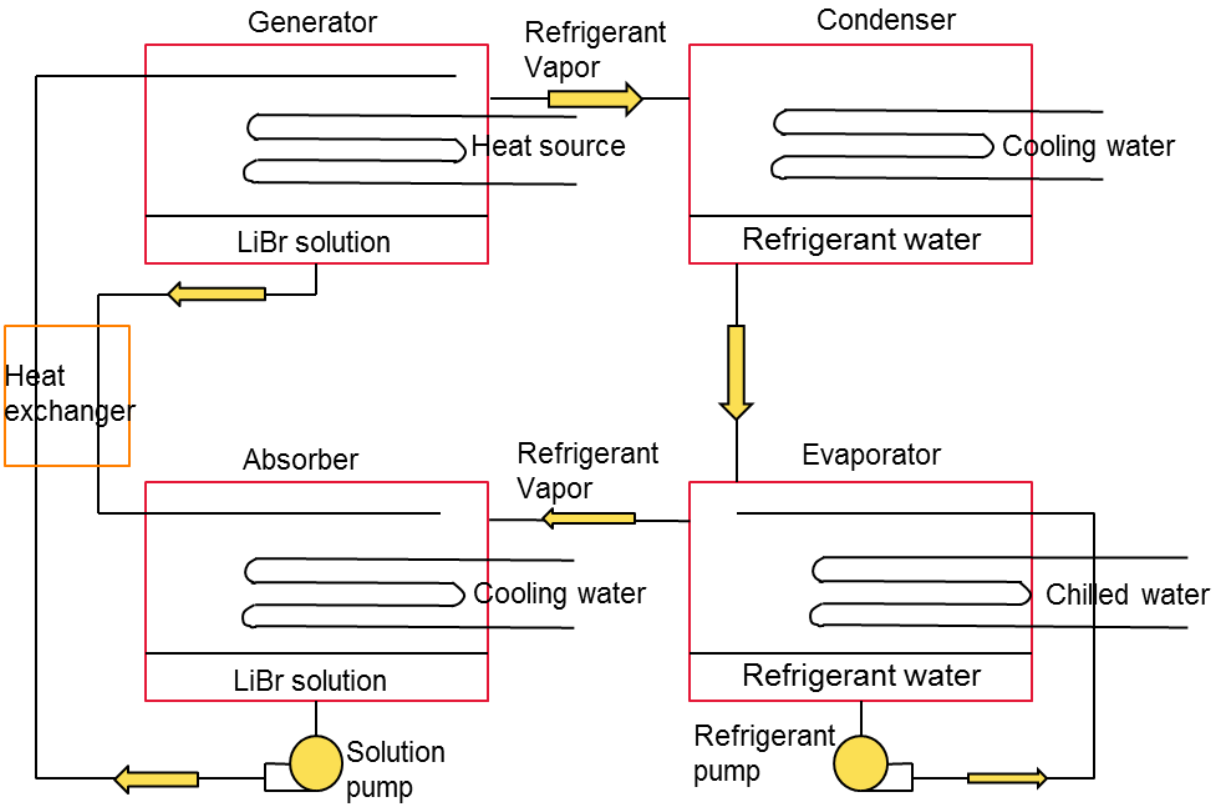

continuously removed out from the evaporator by the strong lithium bromide in the absorber. The lithium bromide solution is used as the absorbent and water is used as the refrigerant.

Figure 1-1: Illustration of a single-effect Li-Br absorption chiller.

Absorption cooling has attracted a lot of attention as an alternative to conventional vapor compression cooling. Among the components, the absorber is the most important element of the absorption cooling cycle, and its characteristics have significant effects on the entire system's performance. A typical absorber of a conventional Lithium Bromide absorption system includes a bundle of horizontal tubes and drippers. The solution is introduced on the tubes as droplets from the drippers and flows as liquid film on the tubes. This style of falling-film absorber is used in most absorption machines because it has several advantages, such as high heat transfer coefficient, relatively low pressure drop, and a sufficient absorption process compared to other tube arrangements. The absorption phenomena depend on many parameters such as solution flow rate, tube parameters, and surface condition, which governs flow around and between the tubes. Some simplified smooth laminar falling-film models have been done by several researchers (e.g. Islam, 2007, Bredow et. al., 2008).

Even the absorption chiller uses waste heat as the energy resource, the general adoption is still constrained by the low COP. The main barrier of the performance is the heat and mass transfer in the absorber. Scientists and researchers have been working on this issue for decades. Adding additive and using different kinds of tubes have been proven effective in enhancing the system performance and applied in industrial. However, to couple with the heat transfer in other elements of absorption system, the performance of absorber still has a lot of space to improve. Thus our research focuses on a new method to improve the absorption chiller system: the mechanism motion. The mechanism motion was barely used in industrial to enhance the heat and mass transfer. Only very few research was

conducted in this area; however the output seems very prospective. The mechanism motion may increase the heat and mass transfer in an absorber from the following aspects.

1.2 Increase additive performance

Although the additive effect is still in debate, the most accepted theory is that the additive could reduce the surface tension and arouse Marangoni vortex (Frances and Ojer, 2004). Mechanism motion could further break the surface tension, thus make the falling film distribute on the tubes more evenly. Adding mechanism motion may also increase Marangoni vortex intensity and correspondingly increase absorber performance. But, there is barely any literature discussing how mechanism affects the absorption chiller. Different additives have different characteristics, and different kinds of mechanism motion may also affect the additive performance in different degrees. A real experiment is very necessary for understanding absorption additive performance under a vibration situation.

1.3 Using inertia force to help form droplet

Inertia force will be accompanied with mechanism motion. Obviously, the vibration makes equipment move up and down. The moving direction of equipment changes during the vibration. Inertia force appears when the direction changes. When the tubes begin to move from downward to upward, there is still a downward inertia force on the falling film. This inertia force compels the solution move down to next tube.

1.4 Thin out and surface fluctuation

In previous studies, which will be introduced in the literature review in this thesis, researchers conducted various experiments to demonstrate that vibration could reduce the surface tension and film equilibrium (Aoune and Ramshaw 1999; Cheng et al. 2009;

Ellenberger and Krishna 2002; Liu t al.2004). They found films with less thickness were formed and the surface of film introduced some fluctuation during vibration. These two phenomena play positive role in absorption process. A thinner film reduces the heat transfer resistance through the film and a fluctuating surface increases mass transfer across the film liquid-vapor interface. If the LiBr solution remains on the falling film too long after saturation, the system would have no future performance improvement during the absorption and saturation period. With a given flow rate, a thinner film means the droplets fall sooner from the top to the end of the absorber. Making the falling-film droplet fall sooner after it is saturated is one of the investigations in attempt to increase the chiller performance in our experiment. Enhancing heat transfer would benefit the mass transfer correspondingly. In summary, it is expected that "thinning out" the falling film could enhance the heat and mass transfer from several aspects.

Chapter 2 Aims of the Project

The objectives of this research project are to:

i. Develop an active enhancement method for the absorption chiller technology that might enhance the coupled heat and mass transfer in the absorber;

ii. Construct experimental set-up for conducting experiments under various frequency and amplitude combinations;

iii. Evaluate the heat and mass transfer performance of the absorber in the absorption chiller before and after vibrations.

Since chemical additive is the current practice in absorption chiller technology, Comparisons between the heat and mass transfer enhancement of the absorption chiller with and without solution additive were also conducted.

Chapter 3 Literature review

To gain a better understanding of this issue, we conducted plenty of literature review, including almost all previous research on mechanism motion enhancing sorption liquid, heat and mass transfer enhancement method and the influence from different kinds of additives.

The refrigeration effect is obtained via a heat-driven cycle in which an absorbent auxiliary fluid enables the main refrigerant to complete its refrigeration cycle through absorption process in the absorber. Two absorption systems based on the lithium bromide-water and ammonia-water are among the highly used working fluids in absorption refrigerating systems and consequently, have been the subject of research from different aspects. The absorption phenomenon, technical performance, falling film modeling and sizing (Kim et al. 1995; Yigit 1999; Jeong and Garimella 2002; Nosoko et al. 2002; Babadi and Farhanieh 2005; Seol and Lee 2005; Kyung et al. 2007; Sultana et al. 2007; Bredow et al. 2008; Islam 2008; Lee et al. 2012; Papaefthimiou et al. 2012), as well as the heat and mass transfer enhancement and surface tension reduction (Hoffmann et al. 1996; Kim et al. 1999; Yuan and Herold 2001; Kulankara and Herold 2002; Park et al. 2004; Soto Frances and Pinanzo Ojer 2004; Jun et al. 2010) of absorption refrigeration systems with various designs and sizes have been experimentally and theoretically investigated in the literature. Among these works on absorption refrigeration systems, not all of the aspects received adequate attention. One of the areas that has received limited research efforts is the effect

of vibration mechanism on heat and mass transfer on falling film absorbers used in the real absorption machines.

In recent years, there has been a continuous attempt to improve the relatively poor COP of absorption refrigeration systems by cycle design modification. Generator absorber heat exchanger (GAX) cycles were proposed to reuse the absorber heat to assist generate more refrigerant vapor (Garimella et al. 1996; Rameshkumar et al. 2009; Barrera et al. 2012). In these systems, the absorber heat is supplied to the low-temperature part of the generator and therefore, reduces the external heat source energy consumption. Multi-effect cycles, such as double-effect, triple effect and so on, have been designed to recover the rejected heat of the condenser through additional generators or another cycle (Arun et al. 2000; Tierney 2007; Garousi Farshi et al. 2013). Recently, in order to improve the entrainment ratio of the ejector and enhancing cooling effect inside the evaporator, a flash tank was added between the condenser and evaporator to a solar combined ejector–absorption refrigeration system(Sirwan et al. 2013).

It is true that the COP of an absorption system increases significantly through multi-effect cycles (Gomri 2010), but, there could be serious obstacles in their practical applications, especially in triple-effect machines. Firstly, the solution and additives stabilities could be compromised in considerably high solution temperatures, which also accelerate the corrosion process in chillers (ASHRAE 2010). Secondly, excessive pressure in the first effect generator requires expensive pressure devices (ASHRAE 2010). Thirdly, the overall cost, weight and size of the machine increases significantly due to replication of several components of the same type in the whole unit. Above all, since the total

performance of the system is obtained from both the cycle design and components' performance, therefore, moving toward higher COPs is hinged with the improvement of the two factors, cycle modification and individual components performances, simultaneously. In this work, special attention is paid to the absorber, as the most important component of the system, to identify potential enhancement of heat and mass transfer coefficients, with or without additives, via vibration mechanism, and consequently to increase the efficiency of the whole system without the need for major cycle modification.

3.1 Heat and mass transfer enhancement via active mechanisms

There are many different types of active methods all of which aim to accelerate heat and mass transfer through the motion mechanism. Transfer coefficients were significantly improved in a heat pump in the study by Aoune and Ramshaw (1999) over thin fluid films via rotating disks. Mechanically induced vibration, as another active technique, also was studied in several researches including the study of flow induced vibration effect on heat exchangers by Cheng et al. (2009), and the experimentation of interfacial mixing effect of vibration in absorbers by Tsuda and Perez-Blanco (2001). As another active mechanism, ultrasound vibration enhancement method was investigated by Kiani et al. (2012). Regardless of the type of the oscillating motion, almost in all cases, in presence of vibration, heat and/or mass transfer were improved. More examples of active techniques could be found in the study by Bergles and Manglik (2013). This section is focused on heat and mass transfer enhancement through mechanical excitation or vibration.

3.1.1 Flow-induced vibration

The kinetic energy of a working fluid within a component can generate vibration on its whole body or a specific segment. A unique design of heat exchanger was proposed by Cheng et al. (2009) to transform a part of the energy of the fluid flow into useful vibration on heat exchanger tubes. This vibration aims to firstly, improve the heat transfer coefficient, and secondly, decrease the fouling resistance in the tubes. The newly designed heat transfer apparatus consists of elastic tube bundles (A, B, C, and D) of looped curved beams, which a couple of them are positioned horizontally in layers above one another in the heat exchanger chamber. Two solid joints (E, F) connect these semicircular beams together to create a closed loop of the fluid inside the bundle (as shown in Fig. 3-1)

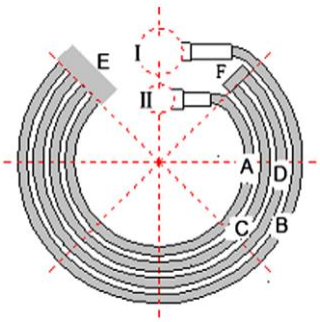

Figure 3-1: In-plane nonlinear heat transfer device. Source:(Cheng et al. 2009)

Dynamic sub structure method was utilized to analyze the vibration of the tube bundle after which the first six natural frequencies of the system were obtained. Three of these modal shapes were out-plane and the rest were in-plane vibrations. In the experimental study, the convective heat transfer coefficient α was measured with the Newton's law of cooling:

$$\alpha = \frac{\mathrm{Q}}{\mathrm{F}\Delta\mathrm{t}} = \frac{Q}{F(T_w - T_f)} \qquad (3\text{-}1)$$

Where Δt is the difference between the tube wall temperature and the average fluid temperature between the shell and heat transfer bundles. F is the heat transfer area, T_w is the average value of 28 points of temperature measurements on the tube surface, and T_f is the average between inlet and outlet temperatures of the shell side fluid. The heat transfer rate, Q, could be obtained by knowing the specific heat of the fluid under a constant pressure, mass flow rate, and the inlet and outlet temperature of the shell side fluid. In this experiment, the shell side fluid entered the chamber from its bottom and after passing the heat transfer tube bundles, flowed out from the top of the chamber. The vibration of the tube bundles in this study was due to the shell side fluid pulsations; therefore, there was a weakening effect in vibration from one horizontal tube to the upper from the bottom to the top of the chamber. In the same conditions, the convective heat transfer coefficient α obtained from flow-induced vibrating tubes was compared with tubes in the fixed position. For different mass flow rates with associated Reynolds numbers in the range of about 65 to 450, the experimental results showed significant heat transfer improvement of vibrating tube bundles in comparison to fixed tube configuration.

3.1.2 Vibration of a heat pipe

In another study, Chen et al. (2013) experimentally studied the effect of horizontal longitudinal vibrations on heat transfer in a grooved cylindrical copper heat pipe (passive heat dissipation devices) with frequencies of 3, 4, 5, 6 and 9 Hz, and amplitudes of 2.8, 5, 10, 15, 20 and 25 mm (0.11,0.20,0.39,0.59, 0.79 and 0.98 in). Their experimental setup consisted of heat pipe, cooling, heating, vibrator, data collection systems, thermocouples,

insulations, flow meter, DC power supply and thermo-regulated bath. (as shown in Fig. 3-2)

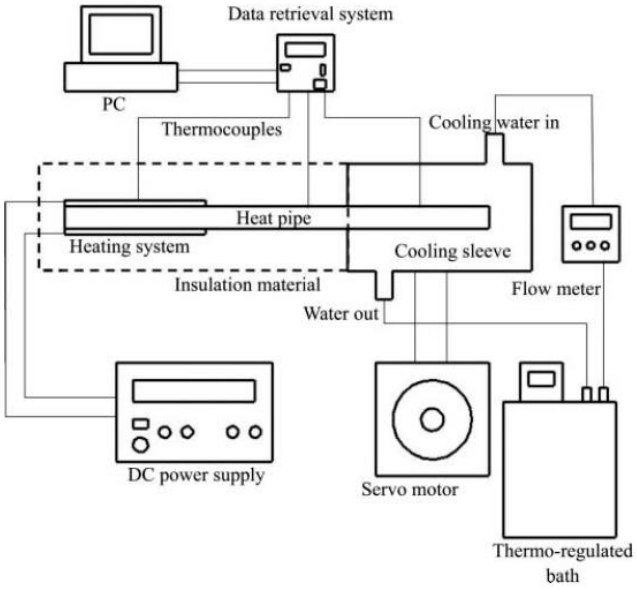

Figure 3-2: Experimental set-up. Source: (Chen et al. 2013)

Heat pipe was positioned horizontally between the heat source section (evaporation section) and condensation section. Thermocouples of type-K were installed in each 40 mm (1.57 in) on the surface of the heat pipe to monitor any changes in temperature before and during the vibration process. The arithmetic averages of these recorded temperatures of that division are the evaporation and condensation section temperatures. They found that the increases in amplitude and frequency decreased the thermal resistance of the heat pipe. The vibration energy of up to 500 mm^2Hz^2 (0.7750 in^2Hz^2) has a proportional effect on increasing the heat transfer of the heat pipe, but beyond this value there was a decrease in the heat transfer rate enhancement per unit of vibrational energy. Results in that paper show an increase of about 215 % in heat transfer only between the frequency of 3 and 9 Hz and amplitude of 2.8 mm (0.11 in) under the condensation temperature of 30 ˚C (86 F). A 900%

increase in the maximum heat transfer rate enhancement was recorded between the amplitude of 2.5 mm (0.10 in) and 25 mm (0.98 in), and frequency of 3 Hz under the condensation temperature of 30˚C (86 ˚F).

3.1.3 Vibration of a wire and a coated metal

Lemlich (1955) experimentally studied the effect of vibration on heat transfer coefficient between the air as the fluid (film over the wire), and three wires of different diameters. In this experiment, wires were concurrently subject to vibration in the range of 39 to 122 Hz, and electrical current for heating purposes. Natural convection between the air and heated and vibrated wire was measured through the measurement of the temperature, with a calibrated thermocouple, in the middle of the wire. Within the specific range of amplitude in this work, heat transfer coefficient improved as the frequency and amplitude increasing. It also showed that the heat transfer enhancement is more significant when the temperature difference between the wire and air is small. Its reason, as explained in that paper, is that higher natural convection causes a higher level of disturbance. In this context, the increased disturbance due to the increase in vibration excitation accounts for a lower proportion in whole existing disturbance around the fluid films. The researcher also proposed, but not proved, that the vibrating wire allows the air to create a stretched film over the entire path of the motion, and therefore, air does not follow the wires back and forth movement.

Lemlich and Levy (1961) investigated the effect of vibration on mass transfer coefficient through the vibration of a coated metal of Aluminum or steel covered with naphthalene or d-camphor. The sublimation of this substance into the room air through

mass transfer was the main mechanism of the experiment. The vibrating metals were suspended within a cradle from a main wire in the room area. Main wire itself was in contact with an oscillator to receive the vibration necessary to the test runs. After each run of the test, the specimens were reweighted and the diameters were re-measured. The mass transfer coefficient increased due to this vibration of up to 660%. Influence of the amplitude increase was more than that of frequency.

3.1.4 Vapor-liquid interfacial vibration

Another active mechanism to enhance mass transfer is the direct application of vibration on surface area of the falling film of solution. In a study by Tsuda and Perez-Blanco (2001), an active enhancement technique to improve the overall absorbing performance of the LiBr-water solution-based absorber with a special focus on enhancing, through vibration, of the interfacial mixing between the refrigerant and the solution in the absorber was devised and tested. As illustrated in Fig. 3-3, the proposed absorber consists of a vertical plate over which the working fluid flows; this fluid has a complete contact with the plate from both side; a screen which is meshed with thin vibrating wires is positioned with a distance almost equal to the film fluid thickness.

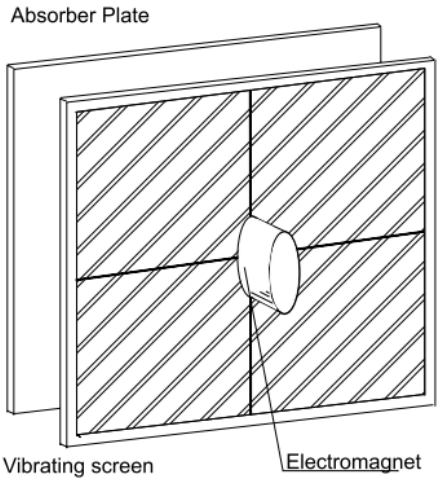

Figure 3-3: Schematic of the vibrating plate mechanism. Source:(Tsuda and Perez-Blanco 2001)

The whole apparatus seems to be capable of simulating the condition exists in an absorber. The effect of vibrating screen on mass transfer rate was obtained through comparison with the case of absorption rates under no vibrating screen. While pressure was kept constant at 5.99 mmHg (0.24 inHg), different mass transport rates were resulted from any different combination of Reynolds number, frequency and amplitude. With amplitude of vibration of 0.2 mm (0.008 in), mass transfer has its highest rate around frequency of 40 Hz in low Reynolds numbers in the range of 20 and 60, and around 60 Hz in high Reynolds numbers between 80 and 300. At configuration with Reynolds number of 80, frequency of 60 and amplitude of 1 mm (0.04 in), a peak value of 14.7 Kg/h-m^2 (348.84 lbs/h-ft^2) was recorded for the refrigerant mass flux into the solution plate. This shows around 150 percent improvement in respect to mass flux rate of 5.9 Kg/h-m^2 (140.01 lbs/h-ft^2) at Reynolds number of 80 without vibration. A limitation of this method would be the physical presence of the screen wires as an obstruction; screens with more vibrating wires,

to intensify the mixing effect, would obstruct the contact between the gas and fluid and deteriorates the absorption rate, on the other hand, screens with a lot of free area could not mix the solution interface effectively.

3.1.5 Vibration of LiBr-H2O falling film absorber

As a rare example, the effect of vibration on transfer coefficients in an absorber apparatus with horizontal tubes and LiBr-water solution as working fluid was experimentally tested by Kostin and Gorshkov (1990). According to the literature review conducted by Kostin and Gorshkov on similar processes, vibration could improve the heat and mass transfer coefficients. The hermetically sealed experimental set-up of the absorber consisted of a single row of horizontal tubes arranged one above the other, through which cooling water flowed to remove the heat of absorption. LiBr-water solution was sprayed down on tube bank and flowed down into two wells at the bottom of the tube tank. Heaters in the wells separated the water from solution through evaporation process, and caused the remains of strong solution. This solution then passed through a heat exchanger which removed the excessively generated heat due to heaters in wells. The heaters' power in the wells was varied to control the steam flow rate over the tube bank in this experiment. To complete the circulation process, the solution coming out of the heat exchanger, then, was pumped to the sprayers. The absorber apparatus was subjected to vibration after which a set of parameters were measured:

Variation of the main parameters in the course of experiment				
Absorption Pressure pa (psi)	Strong solution concentration %	Spray mass flow rate kg/hr/m (lb/hr/ft)	Strong solution temperature ˚C (˚F)	Cooling water ˚C (˚F)
666.61 to 2666.44 (0.097 to 0.387	54-60	500-960 (335.984-645.090)	30-50 (86-122)	5-36 (41-96.8)

Table 3-1: Parameters for the LiBr-water heat and mass transfer experiment

As a result, the effect of mechanical vibration was found beneficial on improving the absorption process. In the test an average enhancement of 15% was reported for heat transfer in the absorber apparatus.

3.1.6 Vibration of an absorption chiller

Liu Y. L. (2004) used vibration test to emulate a working absorption chiller on a boat in motion. A vibration generator was applied to mimic the sea wave effect on the absorber. The test-rig included the signal generator, vibrator, absorber, generator, data collector, and so on. The experiments were conducted for both static and vibrating conditions. With other variables in the system remained the same, the flow rate of the weak solution, vibration frequency, and inclination angle were modulated to investigate the impact of vibration on heat and mass transfer enhancement of the absorber. The results are reproduced in Fig. 3-4.

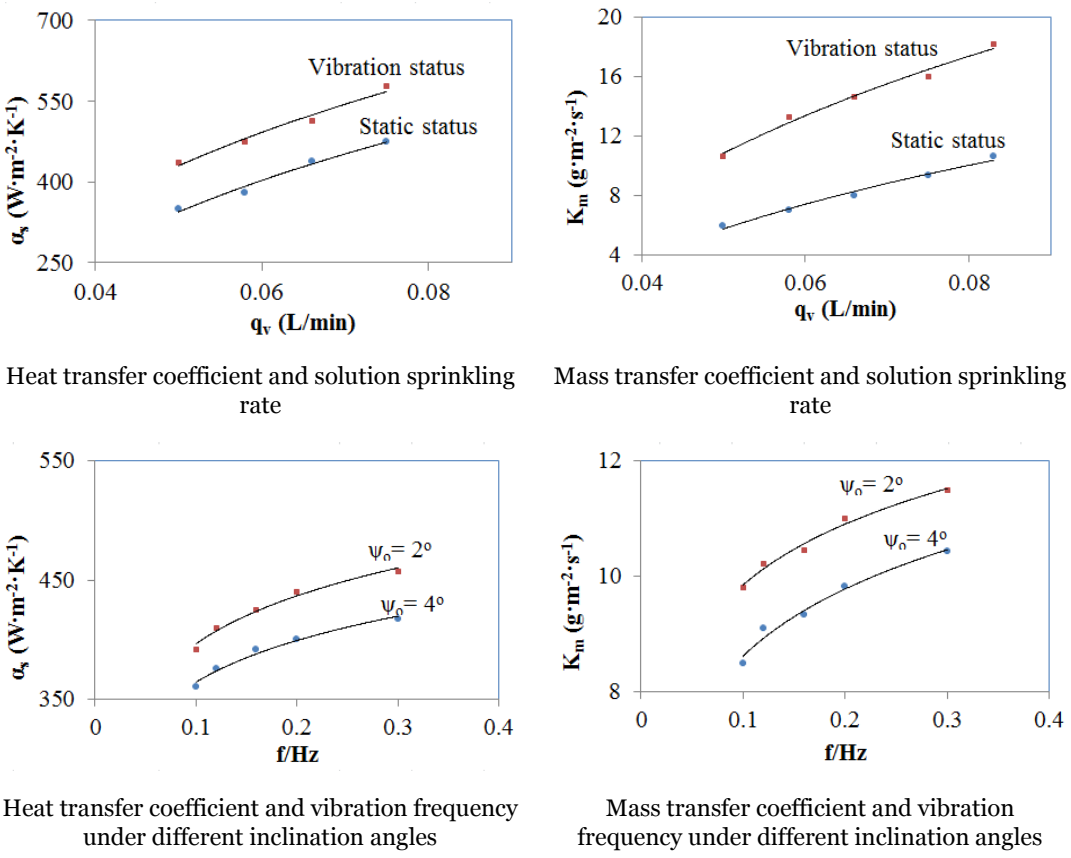

Heat transfer coefficient and solution sprinkling rate

Mass transfer coefficient and solution sprinkling rate

Heat transfer coefficient and vibration frequency under different inclination angles

Mass transfer coefficient and vibration frequency under different inclination angles

Figure 3-4: Heat and mass transfer comparison (reproduced from Liu Y. L. 2004)

The upper two figures show the heat and mass transfer coefficient under vibration status and normal static status. They demonstrated that vibration remarkably enhanced the heat and mass transfer. The enhancement of mass transfer is notably high, almost 100% higher than static status. Heat transfer enhancement, which is not as high as mass transfer, also has a 20% increase. The bottom two figures reflect the relationship between heat/mass transfer and the frequency/inclination angle. With the same inclination angle, increase of frequency below 0.4 leads to the increase of both the heat transfer and mass transfer. The reasons are that the increase of vibration frequency, on the one hand, amplifies the radial and tangential speed of the liquid on the absorber tubes and therefore enhances the heat

convection, and on the other hand, speeds up the fluctuation of the tube surface and the replacement of the saturated vapor/liquid close to the tube surface. However, the heat and mass transfer is better when the inclination angle is relatively lower. From the plots, we could see that the 2-degree slope has a better performance than the 4-degree one. The authors concluded that there was a critical value for both vibration frequency and amplitude (inclination angle in this case). The absorption will enhance at the beginning of vibration, but when vibration reaches the critical value, the absorption process will be weakened. Another point that should be considered in this paper is, the frequency is very low in this experiment because the waves on the sea are not controllable and the vibration is subject to the boat stability.

3.1.7 Ultrasound vibration

Ultrasound vibration, as another active mechanism to intensify the transfer coefficients in different devices, has also been tested experimentally. Melendez (2010) attempted to develop an air scrubbing system, a countercurrent single stage scrubber, capable of influencing the gas-liquid mass transfer with Nano chemistry, and then to investigate the enhancement potential of ultrasound vibration on mass transfer phenomenon in the designed apparatus. To test this potential, Melendez, conducted a number of experiments with and without the application of ultrasound action on the designed apparatus. This device consists of a cylindrical container in the middle of which some horizontal perforated sieve plates were installed. The air and water then were blown and pumped into the scrubber to start the process of the absorption of oxygen into water. In this cylindrical container, the gas entered from the bottom of the apparatus and was in contact with flowing water over sieve plates. The remaining gas, after absorption, exited

from the top. The enhancement was measured by comparing the amount of oxygen absorbed in the scrubber in the cases of with and without ultrasound vibration. Although a literature review conducted by Melendez showed that ultrasound might enhance the liquid phase mass transfer coefficient, experimental results completed by Melendez failed to present any significant improvement of the mass transfer under the application of ultrasound vibration.

As another more recent example, the effect of ultrasound intensity and distance from the transducer source on heat transfer coefficient between a coolant medium and a copper sphere was experimentally investigated by Kiani et al. (2012). The experimental setup consists of a stainless steel tank under which six piezoelectric transducers were installed and one ultrasonic generator. The coolant medium (a mixture of ethylene glycol and water at -10 ˚C (14 ˚F) then was exposed to the frequency of 25 KHz and intensities of ultrasound of 0, 120, 190, 450, 890, 1800, 2800, 3400 and 4100 W m^{-2} (11.148, 17.652, 41.806, 82.684, 167.226, 260.129, 315.871 and 380.903 W ft^{-2}) to measure the heat transfer trend on the surface of the copper sphere. The phenomenon of heat transfer enhancement was attributed to (1) the propagation of the ultrasonic waves to intensify the mixing effect, and (2) the creation, growth and collapse of bubbles in the liquid due to mechanical force introduced by ultrasonic vibration. They found that the application of the ultrasound with the intensities of 120, 190 and 450 W m^{-2} (11.148, 17.652, 41.806 W ft^{-2}) were more effective to increase the cooling rate and decrease the cooling time. Higher intensities of ultrasound vibration could create a considerable heat on the surface of the sphere and the medium, which adversely affected the heat transfer.

Sources	Method	Interactive media	HTE	MTE	Apparatus	Amplitude	Frq
Chenget al. (2009)	Flow-induced vibration	Water-heated tubes	Around 250 % enhancement in Heat transfer coefficient	N/A	Newly designed heat exchanger with rows of in-plane curved tube bundles	N/A	8.75 Hz for the first mode of vibration
Chen et al.(2013)	Vibration of a heat pipe	Distilled water and copper heat pipe surface	Up to 900 % enhancement in maximum heat transfer rate	N/A	Integrated Heat pipe device	2.8, 5, 15, 20, 25 mm (0.1102, 0.1968, 0.3937, 0.5905, 0.7874 and 0.9842 in)	3, 4, 5, 6, 9 Hz
Lemlich (1955)	Vibration of wires in contact to air	Air-Heated wires	Up to 400 % enhancement in heat transfer coefficient	N/A	Horizontal heated Nichrome wire under sinusoidal vibration created by a buzzer	0.055-0231 inch (1.397-0.58674 mm)	39-122 Hz
Lemlich and Levy (1961)	Vibration of coated cylindrical metals	Naphthalene or d-camphor - room air	N/A	Up to 660%	Assembly of wire, oscillator, amplifier and cradle	Double amplitude: 0.46 to 7.66 mm (0.01811024 - 0.3015748 in)	20-118 Hz
Tsuda, Perez-Blanco (2001)	Solution-gas interfacial mixing due to the vibration of a screen of wires	Coolant water tubes-Lithium Bromide water solution-water vapor	N/A	Up to 150 percent depending on different situation	Plate absorber equipped with a vibrating screen	0.2-1 mm	20-100 Hz
Kostin and Gorshkov	Vibration of the absorber apparatus	LiBr-water solution and water vapor	15 %	N/A	falling-film absorber apparatus with horizontal tube bank	2A = 3 mm (0.11811 in)	14 Hz
Liu and Xu, (2004)	Vibration (swing)		20%	90%	Absorber Chiller equipped with a Vibration Generator	2-4 degree	0.2-0.6 Hz

Melendez (2010)	Ultrasound vibration	Oxygen and water	N/A	Non	Single-stage, Sieve plate scrubber for lab purposes	N/A	20 KHz
Kiani, Sun and Zhang	Ultrasound vibration	Ethylene glycol and water mixture	Between 2 and 400 %	N/A	Suspended copper sphere in fluid tank in vicinity of a transducer	N/A	25 KHz

Table 3-2: Summary-heat and mass transfer enhancement via vibration

Note: HTE- heat transfer effect, MTE- mass transfer effect, Frq- frequency.

Table 3-2 compared the reported heat and mass transfer enhancements due to the active mechanism of vibration in the discussed literature including the amplitude and frequency of the vibration. Collected research works in this table presented completely different approaches for testing the effects of vibrations on transfer coefficients. Their testing apparatus, sources of vibration, types of vibration, frequencies and amplitudes, temperatures, measurement devices, and mediums varied from one experiment to the other. From Table 3-2, the vibration type could be roughly divided in two groups of low frequency (0-150 Hz), and ultrasonic vibration (above 20 kHz). For frequencies in the range of the 0-150 Hz, the amplitude is between 0.2 to 25 mm (0.008 to 0.984 in). For both categories of vibration, considerable heat transfer improvements were reported with the maximum heat transfer improvement of 900% obtained from the effect of vibration on a heat pump. For other studies, which operation mechanism bears more resemblance to absorbers, improvement of around 300% was reported. Unlike the heat transfer, there are fewer studies on the effect of vibration on mass transfer coefficient. However, from these research works, a good number of them showed considerable mass transfer improvements in the presence of an oscillatory source.

3.2 Passive techniques in absorbers for heat and mass transfer enhancement

Passive techniques are more developed, proved useful and widely used to enhance heat and mass transfer in absorbers. Their application in falling film absorbers with horizontal tubes could be divided into two main categories as (1) tube surface transmutation and (2) solution additives. From these, increasing the wettability of tubes, reducing surface tension and increasing the mixing effect in the solution are main sought-after outputs. The positive enhancement effect of passive techniques including the surface treatments and roughness, inserted enhancement devices, swirl-flow devices and geometrical modifications have been tested on variety of different components and devices(Bergles and Manglik 2013). Not surprisingly, the effect of the surface treatment and roughness on transfer coefficients of falling film absorbers also could be found in literature (Hoffmann et al. 1996; Park et al. 2004). In this section the effect of solution additives on the falling film absorbers with horizontal tubes will be reviewed. Additives are widely used in commercial absorption chillers and are relatively easier and less expensive to apply than other passive methods.

While additives increase the mixing effects in the working solution through Marangoni effect, they increase the wettability through surface tension reduction. The surface tension of LiBr-H2O and distilled water was tested with four different additives and two different solution concentrations by (Kulankara and Herold 2002). The drop weight method was used to measure the surface tension through weighing the drops falling from a small diameter nuzzle of a stainless steel tube attached to a liquid container.

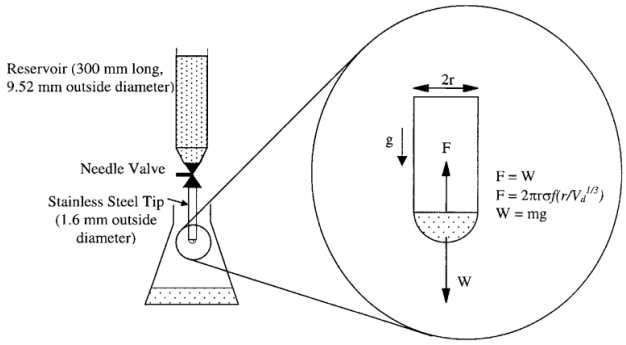

Figure 3-5: Surface tension measurement apparatus. Source: (Kulankara and Herold 2002)

The formula from Harkins (1952) was used to obtain the surface tension:

$$W = 2\pi r\sigma f(\frac{r}{V_d^{\frac{1}{3}}}) \qquad (3\text{-}2)$$

Where σ is the unknown surface tension, W is the weight of the drop falling on the apparatus collection tray, r is the tip's radius, and V_d represents the volume of the drop. The remaining water at the tip when a drop falls was taken into account by the Harkins Brown correction factor of f-function. Based on the measurements, they found considerable surface tension reduction due to the additives in the solution.

A more germane understanding of the enhancing effect of additives to absorber performance is obtained through direct measurements of heat and mass transfer rates. Kim et al. (1999) experimentally studied the effect of eight pairs of solution and additive mixtures of 50, 60, 68 and 70% and n-octanol, 2-octanol, 3-octanol, and 2-ethyl-1-hexanol respectively on mass transfer in a newly designed simple stagnant pool absorber. From these eight combinations, four of them consisted of the same solution of Lithium Bromide and water vapor with different additives and the rest, have the same additive of 2-ethyl-1-

hexanol and different solution (as shown in Table 3-2). The procedure consisted of weighing carefully the solution, with desired amount of additives, before and after the experiment, to find the absorbed water vapor in each 3-minute absorption period in the solution. During the experiments, a considerable surface turbulence was observed from the transparent façade of the apparatus during absorption process with the use of additives. As a result, considerable mass transfer enhancement was recorded with the use of additives.

In another example, the 2EH and 1-octanol additives effect on the heat transfer enhancements in a LiBr falling film solution absorber was experimentally tested on two types of plain and treated horizontal tubes by Hoffmann et al. (1996). The experimental setup consists of horizontally arranged tubes with the solution dripping over from the top. Then the gathered solution was pumped from the bottom of the pool and recirculated to complete the process. They obtained a total *U* value for the absorber from the formula of:

$$\dot{Q}_{total} = U_{total} A \Delta T_{logmean} \qquad (3\text{-}3)$$

$\Delta T_{logmean}$ is the mean logarithmic temperature difference between the equilibrium temperature of the solution and the cooling water temperature. U_{total} is the total heat transfer coefficient of the absorber which consists of the effects of solution and cold water heat transfer coefficients, α_{sol} and α_{cw} :

$$\frac{1}{U_{total}} \approx \frac{1}{\alpha_{cw}} + \frac{1}{\alpha_{sol}} \qquad (3\text{-}4)$$

Total heat flux $\dot{Q}_{total}$ is calculated from:

$$\dot{Q}_{total} = \dot{m}_{cw} c_{cw} (T_{cw,out} - T_{cw,in}) \qquad (3\text{-}5)$$

Where, $\dot{m}_{cw}$ is mass flow, $T_{cw,out}$ and $T_{cw,in}$ are temperatures in inlet and outlet respectively and c_{cw} is specific heat capacity of cooling water. It is experimentally tested that the heat transfer of cold water inside tubes was much higher than the solution side. Therefore, the restricting factor here would be the heat transfer of the solution. Under constant heat transfer of the cold water inside the tubes, any change in the U_{total} is directly related to the heat transfer improvement of solution. Adding the additives could possibly improve the total heat transfer coefficient by 100%.

A simultaneous heat and mass transfer enhancement due to an additive is presented by Park et al. (2004). In order to increase the systems' performance, as part of their research, the effect of additive octanol (400 ppm) was experimentally tested on heat and mass transfer in an absorber with horizontal tubes. Their experimental setup consisted of the absorber, pumps and distribution devices, heat exchanger, coolant fluid, circuit and generator. The absorber had 24 horizontal tubes arranged in a vertical column. 24 local temperature measurements for coolant fluid and 2 solution temperature measurements at inlet and outlet were installed. The inlet temperature of coolant was kept constant at 32.5 ˚C (90.5 ˚F), and the absorption performance determined the outlet temperature variations. Then, heat transfer coefficient was calculated from the coolant temperature differences, and mass transfer was obtained from direct weighing of the solution fluid. As a result, they found considerable enhancement of heat and mass transfer on plain horizontal tubes.

Solution	SC %	Additives	HTE %	MTE %	STR %	ADC ppm	Remarks
Kim et al. (1999)							
LiBr + H_2O	50	n-octanol	-	358.33	-	200	CC

LiBr + H2O	50	2-octanol	-	316.67	-	200	CC
LiBr + H2O	50	3-octanol	-	308.33	-	400	CC
LiBr + H2O	50	2-ethyl-1-hegxanol	-	333.33	-	200	CC
LiBr + H2O	60	2-ethyl-1-hegxanol	-	156.41	-	200	CC
LiBr + H2O +$HO(CH_2)_2OH$ (LiBr/ $HO(CH_2)_2OH$ = 4.5 by mass)	68	2-ethyl-1-hegxanol	-	200.00	-	190	CC
LiBr + H_2O + LiI (LiBr/LiI = 4 by mole)	60	2-ethyl-1-hegxanol	-	202.78	-	200	CC
LiBr + H_2O + $ZnCl_2$ ($LiBr/ZnCl_2$= 1 by mass)	70	2-ethyl-1-hegxanol	-	181.25	-	300	CC
Kulankara and Herold (2002)							
LiBr + H2O	53	2-ethyl-1-hegxanol(2EH)	-	-	56.53	106	CC
LiBr + H2O	53	2-methyl-1-hexanol (MHX)	-	-	60.63	135	CC
LiBr + H2O	53	3,5,5-trimethyl-1-hexanol (TMHX)	-	-	57.83	58	CC
LiBr + H2O	53	3-phenyl-1-propanol (PHPP)	-	-	54.21	>1500	CC
LiBr + H2O	60	2-ethyl-1-hegxanol(2EH)	-	-	55.93	55	CC
LiBr + H2O	60	2-methyl-1-hexanol (MHX)	-	-	60.63	58	CC
LiBr + H2O	60	3,5,5-trimethyl-1-	-	-	56.22	15	CC

		hexanol (TMHX)					
LiBr + H2O	60	3-phenyl-1-propanol (PHPP)	-	-	55.22	>500	CC
Hoffman et al. (1996)							
LiBr + H2O	56	2-ethyl-1-hegxanol	100	-	-	40	CC HTE is average enhancement in α_{sol}
Park et al (2004)							
LiBr + H2O	61	Octanol	406.56	376	-	400	HTE is enhancement in Nusselt Number Nu

Table 3-3. Summary heat and mass transfer via additives

Note: HTE- heat transfer effect, MTE- mass transfer effect, STR- surface tension reduction, SC- solution concentration, ADC- additive concentration, CC-critical concentration

Table 3-3 collects the most relevant efforts on improving the transfer coefficients of falling-film absorbers through the usage of solution additives. LiBr-water solution with two additives of 2EH and Octanol is dominant working fluid. Research works in this table are more comparable than the information in Table 3-2, since most of them are experiments on falling film absorbers with horizontal tubes. Still, the operation parameters (e.g. the temperature, pressure and solution flow rate during the test), the purity of additives, geometry, size and material of the absorber are the factors that might cause the results variations which were not investigated in this review.

3.3 Compound techniques in falling film absorbers

The exercise of two or more heat and mass transfer enhancing techniques in a machine is known as a compound method. Studying transfer coefficients enhancement in falling film absorbers is further complicated with the application of compound methods, especially when many of the enhancing techniques have not yet been tested individually. Nevertheless, a few existing compound techniques presented in the literature, may not explicitly named as compound method, could provide a ground toward the development and eventually, implementation of these techniques in real machines.

A unique attempt to study the heat transfer coefficient improvement due to the tube surface roughness together with solution additives is presented by Hoffmann et al. (1996). Although their apparatus is a falling film horizontal tube heat exchanger, its geometry composition is similar to commercial absorbers. With additive concentration of 80 ppm of 2-ethyl-1-hexanol in the solution of LiBr-water, depending on mass flow rate, on knurled surface tubes, they reached 55 to 85% of improvement in heat transfer coefficient.

Park et al. (2004) later presented another work of the same type by combining the effects of surface roughness and additives. Tube surfaces were roughened with micro-scale hatches of 0.39 – 6.97 μm (15.354 to 274.410μin), and normal Octanol with a concentration of 400 ppm was used as the solution additive. Results showed significant improvement of the absorption performance of 4.5 times for the roughened tubes in presence of the solution additives than that for the plain tubes without the usage of additives.

3.4 Discussion

Application of active, passive or compound methods in a falling film absorber with horizontal tubes and LiBr-water as working solution, leads to different levels of improvement, or possibly deteriorations, of these two transfer coefficients. The similar heat and mass transfer enhancements found in the literature due to the vibration could be executed in falling film absorbers. Vibration of tubes potentially enhances heat and mass transfer. It disturbs the solution bulk and solution-vapor interface which improves the mixing effect, diffusivity and eventually mass transfer rate in solution bulk. This theory could be better supported by considering the relatively high viscosity of LiBr-H2O solutions. This viscosity is the reason for the entire film of solution disturbance by the vibration movement.

Vibration movement path could be divided in three general forms of up-down, right-left, or circulatory paths, regardless of which, from one hand, the film solution on the tubes tends to keep its initial moving path due to its inertia force, and from the other, is dragged by the tube movement path due to the friction force of the tube surface. However, its real movement behavior falls somewhere in between. Namely, there would be constant scrubbing between tube wall and solution bulk, and in the meanwhile, the solution bulk undergoes a disturbance due to the vibration movement. This mechanism increases the heat transfer coefficient between the tube wall and solution bulk, and concurrently encourages the mixing effect. Naturally, this contention, though is true to the best of the knowledge of authors, needs to be proved via theoretical and experimental tests.

3.5 Concluding Remarks

Investigating the development of active enhancement mechanisms for heat and mass transport processes in absorption devices is an essential step prior to onset of experimentation and modeling to provide design tools for any of these techniques. In this thesis, a literature review was carried out with the aim to firstly identify the potential of heat and mass transfer enhancement in absorbers and secondly, to consider the simultaneous application of an active mechanism with a widely used passive technique. The enhancement potentials of each individual technique of vibration and solution additives were described and summarized. After each technique reviewed, experimental conditions and results were gathered in tables to provide a qualitative and quantitative comparison. Based on the reviewed literature, it was hypothesized that a great enhancement potential in heat and mass transfer of the falling-film absorbers with horizontal arrangement of tubes is obtainable by combining vibration effect, as an active mechanism, with solution additives such as 2EH and Octanol. Although a considerable heat and mass transfer enhancement due to vibration could be expected within the schema of a promising prospect, the current studies did not provide a comprehensive and consistent conclusion on the approach, mechanism and performance that support a generalization in falling film absorbers, more research is needed to understand the interchangeable effect in terms of the nature and the magnitude of the simultaneous use of this active method with passive techniques in falling film absorbers with horizontal arrangement of tubes.

Chapter 4 Lab Construction

This part focuses on the lab introduction and the operation sequence. The objective of the project is to investigate the impacts on absorption chillers with mechanism enhancement. In this part, we illustrate the apparatus which could be used to develop a model of heat and mass transfer in absorber. And we also state the challenges which are, the fulfillment of mechanism motion to driving extra heat and mass transfer in absorber, and the measurement of the variables and the stable & repeatability. To explain how we overcome the challenges, we demonstrate the detail of the equipment for absorption chiller, vibrator and auxiliary water loop system and how they work in the experiment. This part provides information of mechanism experiment setup and test methodology for the researchers in the same area who may conduct related work.

The structure of a Li-Br absorption chiller is illustrated in Fig. 1-1. Among the four main components (i.e. a generator, a condenser, an evaporator, and an absorber), the absorber is a key component that significantly impacts the overall performance of chiller. By continuously removing the boiled vapor out of the evaporator, the absorber creates a required low-pressure in the close loop and ensures the continuous stability of the system. Its structure and performance determine the overall size, capacity and efficiency of a chiller. Absorber performance also affects the unit cost and operating economics. Therefore, improving the performance in terms of heat and mass transfer efficiency in an absorber is an important issue facing the academia.

4.1 Experimental challenges

It is expected that, with the designed test-rig and experiments, we could provide solid data with a big range of vibration amplitude and frequency and operation parameters to identify the relationships between the heat and mass transfer and vibration amplitude, vibration frequency and other influencing factors. The comprehensive data collected from the test-rig could be used to develop modeling tools to quantify the vibration effect on absorption chillers. This analysis will fill the blank of heat and mass transfer of horizontal-tube falling film sorption system.

There are challenges for the constructing the test-rig:

i. Mechanism motion and its fulfillment: mechanism motion includes basically vibration and rotation and it can be locally on the absorber or expanded to the whole chiller. Meanwhile, implementation of such a mechanism needs to consider the cost and feasibility. Potential negative impact to the chiller which needs to maintain a vacuum environment should be avoided.

ii. Measurements of the variables: the absorber is one component of the close loop system. To determine the mass and heat transfer, measurements on temperature, flow rate, pressure, and concentration of the strong and weak solution are needed. In addition to the measurement quantity is the quality. Accuracy of the sensors should satisfy the component level and system level heat and mass transfer error analysis.

iii. Stable and repetitive environment: as a close loop system, any change on the four thermal components of the chiller could impact the system operation. To serve Objective-ii, a controllable steady-state condition needs to be maintained

with and without mechanism motion during the operation. A set of artificial thermal source and sink should be constructed and controlled for this purpose.

In the following section, we describe the solutions corresponding to the afore mentioned three challenges.

4.2 Technical analysis and mechanism motion method

As we analyzed before, mechanism motion may reduce the solution film thickness and then reduce heat and mass transfer resistance. At the same time, it may increase the droplet dropping rate by reducing surface tension. On the other hand, mechanism motion may also promote the additive effect and consequently enhance the absorption performance. Since most absorption chillers use horizontal tubes, thinning-out the film should let the motion happen in a vertical direction rather than a horizontal direction. Because a motion in the horizontal direction only makes the film pendulate on the tubes, but does not essentially change the film thickness.

To introduce vibration into our system, we also have many options. One is to vibrate just the tubes in the absorber. However, this kind of design will cause an issue on the vacuum, which is very critical to the normal operation of absorption chillers. A small pressure loss in the absorber will result in big reduction on the cooling performance (Xie et al., 2008). The second design option is using solution to pulse the horizontal tube bundle for vibration. However, it is very hard to control the vibration amplitude and frequency. Considering the complexity involved in absorption chillers, such as dimension, long-time performance, different container arrangement, tubes connection and etc., the best scheme at present is using commercial equipment for conducting the mechanism experiments and

introducing vibration to the entire chiller. Another reason of vibrating the whole chiller is that most commercial products combine the absorber and evaporator, as well as the condenser and generator, into two containers, separately. Having a specially designed absorption system and vibrating only the absorber not only increases the cost, but also prevents the generalization of the findings to commercial products. Meanwhile, separating the absorber from the evaporator into two apart containers increases the pressure drop between them, which is not desired in an absorption system.

4.3 Absorption chiller

Based on the analysis, in this project we choose RXZ (95/85)-1.2ZS type hot water lithium bromide absorption chiller from a brand manufacturer. This chiller contains four main elements: generator, condenser, evaporator and absorber. It also includes air extract instrument, molten silicon tube, solution shield pump and other accessory parts. The detailed parameters are collected in Table 4-1.

Cooling capacity	kW	12	
	Btu/hr	40946	
Coolant water	inlet outlet T	15 to 10^{o}C	59 to 50^{o}F
	flow rate	2 m^3/h	8.8GPM
	pressure drop	2.5mH_2O	3.56psi
	tube diameter	25mm	0.984inch
Cooling water	inlet outlet T	32 to 38^{o}C	90 to 100^{o}F
	flow rate	4.2m^3/h	18.5GPM
	pressure drop	1mH_2O	1.42psi
	tube diameter	25 mm	0.984 inch
Hot water/heat source	inlet outlet T drop	95 to 85^{o}C	203 to 185^{o}F
	flow rate	1550 m^3/h	6824 GPM
	pressure drop	2 mH_2O	2.84 psi
	tube diameter	25 mm	0.984 inch
Electric instrument	Power	3phase - 380V - 50Hz	
	Current	7.7 A	

	Capacity	2.25 kW	
	solution pump	1.3 kW	
	coolant pump	0.4 kW	
	vacuum pump	0.75 kW	
Dimension parameter	Length	1750 mm	68.9 inch
	Width	1100 mm	43.3 inch
	Height	1629 mm	64.1 inch
Operation weight		1200 kg	2646 lbs.
Transportation weight		1000 kg	2204 lbs.
The minimum temperature of coolant water is 5°C/11°F, the minimum temperature of cooling water is 18°C/40°F. Cooling capacity adjustment range is 20-100%. Cooling water and coolant water adjustment range is 60-120%. Coolant water and cooling water, water side fouling factor is 0.086m^2K/kW (0.00049ft^2 F/(Btu/hr.)) Maximum pressure for coolant and cooling water container is 0.8MPa/116psi			

Table 4-1. Specs of the absorption chiller

4.4 Vibration table

In our previous literature review (Behfar et al, 2014), we learned the heat and mass transfer are enhanced in most experiments which introduced mechanism motion The vibration amplitude range is from 0.001 to 2mm while the frequency range is from 2Hz to 200Hz. For a one-ton commercial chiller, a powerful vibrator is needed in order to achieve the requirement of frequency and amplitude combination. The vibration system currently installed includes an ET-50-445 vibration generator, a DA-50 power amplifier, an Amber Digital Vibrancy Control Instrument, a DL acceleration sensor, a B-7000 cooling fan and an air compressor. This equipment has high operability and high load-bearing (3 tons). The frequency range is 5-2700 Hz, and amplitude is from 0-51 mm. The maximum acceleration is 1000 m/s^2. The specs of the vibration generator are provided in Table 4-2. And the pictures of main equipment are shown in Fig. 4-1.

Rated sinusoidal excitation force, peak	50kN	11240lbf
Rated random excitation force	50kN	11240lbf
Impact excitation force, peak	100kN	22480lbf
Frequency range	5～2700 Hz	
Maximum displacement (p-p)	51mm	2inch
Maximum speed	2m/s	6.56ft/sec
Maximum acceleration	1000m/s^2	3280ft/sec^2
First resonance frequency	2400 Hz±5%	
Isolation Frequency	2.5Hz	

Table 4-2 ET-50-445 vibration generator parameters

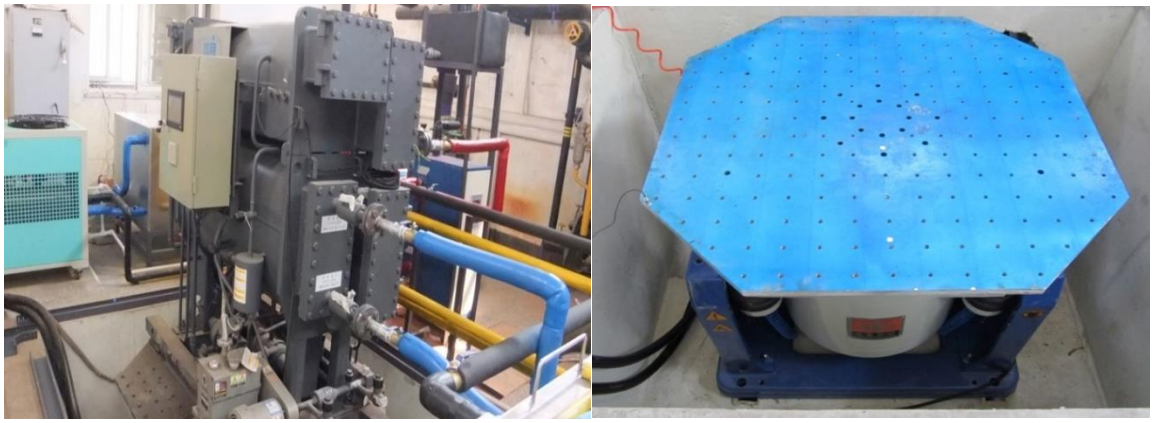

Figure 4-1: Pictures of absorption chiller (left) and vibration table (right)

4.5 Sensing and data acquisition system

Quantification of heat and mass transfer enhancement of the absorber can be indirectly obtained through measurements on the properties of the water and the solution before and after vibration. In the meantime, measurements of the other three parts of the system beside the absorber could also be obtained. As a close-loop system, the heat and mass transfer throughout the components and system should obey the laws of energy and mass conservation. The heat and mass transfer of the entire loop can be utilized to cross-check

the measurement quality. The sensors installed on the system are illustrated in Fig. 4-2. These sensors were not only added around the absorber, but also other main parts of the chiller. Measurements from the evaporator, condenser and generator will also provide valuable data to obtain the information on the cooling performance, mass transfer rate, and the heating source input, etc. A vacuum meter was also installed to monitor the vacuum situation in the absorber.

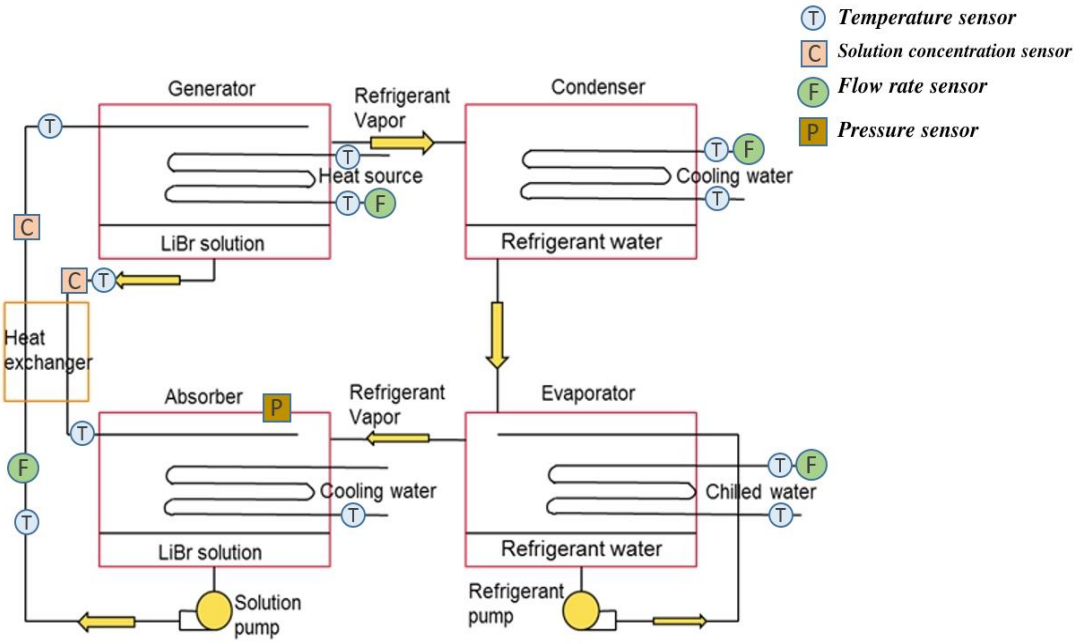

Figure 4-2. System schematic and illustration of the sensors allocation

There are eighteen (18) sensors/meters in addition to the measurements provided by the manufacturer, including:

Eleven (11) temperature sensors on the peripheral water system;

Four (4) flowrate meters with three at the peripheral water loop and one at the weak solution;

Two (2) inline concentration sensors at the strong and weak solution, and

One (1) pressure sensor at the absorber.

There is only one flowrate meter in the solution loop on the weak solution side since the flowrate meter that we used in this project is a turbine flow meter, which incurs significant pressure drop to the system. Thus, it is not recommended to be installed on the strong solution side. However, it was not considered as a concern since the solution loop is a closed loop. In steady-state operation, the mass balance should be observed in the solution loop. Since we monitored the solution concentrations on both strong and weak solution sides (as well as the density) and the volumetric flowrate of the weak solution, we could calculate the flowrate of the strong solution entering the absorber. The temperature data from the measuring sensors was continuously collected with a data acquisition system (model: MX-100). Details of these sensors are summarized in Table 4-3.

	Labels	Note	Remarks / specifications
Temperature	T1	Cold water at the outlet	Platinum thermal sensor, DT-W100 Armored thermal resistors Range: -50°C to +280°C (±0.1 accuracy)/-58°F to 536°F (±0.18 accuracy)
	T2	Cold water at the inlet	
	T3	Condenser cooling water outlet	
	T4	Hot water outlet	
	T5	Absorber cooling water outlet	
	T6	Cooling water inlet	
	T7	Absorber strong solution inlet	
	T8	Absorber weak solution outlet	
	T9	Generator weak solution inlet	
	T10	Generator strong solution outlet	
	T11	Hot water inlet	
Flow rate	Q1	Hot water flowrate	Liquid turbine flow meter Range: 0-5 m^3/h/0-22 GPM (0.5% accuracy)
	Q2	Chilled water flowrate	

	Q3	Cooling water flowrate	Liquid turbine flow meter Range: 0-9 m^3/h/0-39.62 GPM (0.5% accuracy)
	Q4	Weak solution flowrate	Liquid turbine flow meter Range: 0-20 m^3/h/0-88 GPM (0.5% accuracy)
Concentration	X1	Weak solution	Temperature range: 20-120 ^oC/68-248 ^oF (±0.2% accuracy)
	X2	Strong solution	
Pressure	P1	Pressure in absorber	Range: 0-10kPa/0-1.45psi (±2% accuracy)

Table 4-3: Sensor types and the specifications

4.6 In-line concentration measurement

In order to calculate the heat and mass transfer value of the chiller under vibration conditions, in-line concentration measurement sensors were necessary in this project. The in-line measurement for the solution concentration is a new approach in lithium bromide system that we adopted in this project, because it can measure the concentration real-time and allow us to calculate the transient heat and mass transfer analysis.

In-line concentration measurement was rarely used in absorption systems in the literature. Traditionally, with manual measurement, solution needs to be extracted from the system with the assistance of a vacuum pump under the absence of vibration. Considering a negative pressure in the absorption system, it is not a simple matter to leave an opening for abstracting solution sample continuously. Besides, it is labor intensive for sampling solutions. Particularly in this project, the experiments were carried out under vibration, solution sampling was even harder. To overcome these limitations, we used SensoTech® in-line ultrasonic concentration sensor to record the concentration of weak and strong solutions. The operation temperature range is -10-40^{o}C/14-104^{o}F and the accuracy is

±0.2%. The data record frequency for solution concentration measurement is one (1) minute. Based on the knowledge of the research team, this was the first time that an in-line sensor was applied in lithium bromide concentration measurement.

In this experimental system, the ultrasonic concentration detector consists of a controller and two sensors. The sensor is made of stainless steel, comprising an ultrasonic transmitting and receiving device, a built-in high-accuracy temperature measurement sensor, and a communication signal preprocessor. One of the sensors was mounted at the inlet of the absorber to measure the strong solution, and the other was mounted at the outlet of the absorber to measure the weak solution as shown in Fig. 4-3.

Figure 4-3. Photos of the in-line ultrasonic concentration sensor.

Top left, sensor installed on weak solution loop. Top right, sensor installed on strong solution loop. Bottom left, control panel and monitor. Bottom right, electric circuit of data acquisition unit.

We used two different ways to calibrate the sensors and ensure the accuracy of these in-line concentration sensors. One method is using Shanghai Baiyang® lithium bromide solution concentration measuring instruments - glass hydrometers, which can be placed directly into the glass hydrometers to measure its concentration in solution as shown in Fig. 4-4 (left). It is simple and convenient. Another method is using a densitometer and a thermometer to measure the density and temperature of the solution, then using software to calculate concentration values by the density and temperature data. The density is measured by Mettler-Toledo® DA-110M density meter, as shown in Fig. 4-4 (right). This densitometer range is 0-2 g/cm^3 (0-125lb/ft^3) and the accuracy is 0.01g/cm^3(0.624lb/ft^3).

Figure 4-4. Photos of solution concentration (left) hydrometers and (right) liquid density meter

4.7 Thermostatic water loop systems

In order to have a repeatable and fair comparison, except the vibration conditions, all other parameters of the cycle should be maintained as constant as possible. Meanwhile, a

stable thermal sink and source environment should be achieved to ensure that the chiller can maintain a steady-state when we evaluate the performance of the chiller. An external thermal water loop system plays an important role in this matter. Different water loops were constructed to provide controllable temperatures and flowrates at various components, including the generator hot water loop, evaporator chilled water loop, as well as absorber and condenser cooling water loop.

The water loop system for this project was constituted of hot water boilers, pumps, heated water tanks, flanges electric heater, chillers, cooling towers, copper coil heat exchangers, pressure regulators, valves, connecting pipes, pipe elbows, and insulation materials, etc. Fig. 4-5 illustrates the system constructed in the lab and Fig. 4-6 shows photos of the main equipment of the thermostatic water loop system.

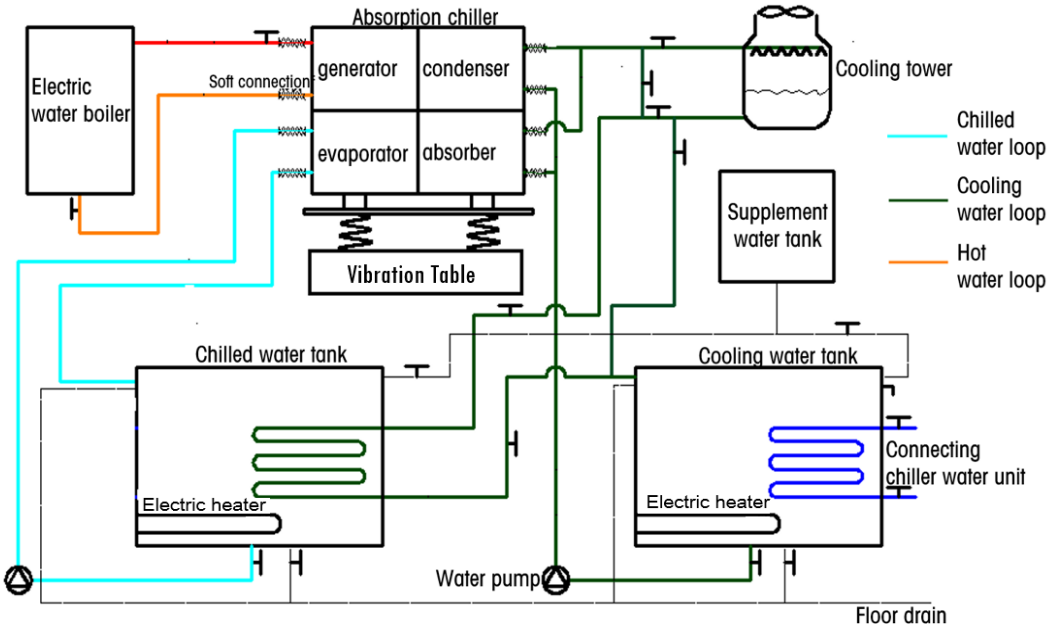

Figure 2-5. Schematic of the test facility

4.7.1 Chiller water unit

The function of the chilled water unit is to chill the water in the cooling tank and to maintain a constant 28-30^{o}C/82-86^{o}F cooling water inlet temperature, continually. For this system, we selected chilled water system with a model of AOY-12500AS. The cooling capacity is 12.5 kW /42,651 Btu/hr. and output water temperature is 7~15^{o}C/44.6-59^{o}F. The chiller has high & low pressure protection, an anti-freeze protection, a voltage/current protection and other safety features.

4.7.2 Water tanks

To create an artificial load and provide constant cooling water to the system, two chilled water tanks of 1m^3/35ft^3 were utilized. The stainless steel chilled water tank and cooling water tank are produced by Tianjin Dingtuo Technology LTD, which are equipped with a drain valve, electric heaters and water level control devices.

4.7.3 Electric boiler

A hot water boiler (with model of CLDR0.024-90/70) was installed to supply hot water to the generator. The power output is 24kW /81,891 Btu/hr., output water temperature is 95^{o}C/203^{o}F, backwater temperature is 85^{o}C/185^{o}F, and the maximum water flow rate is 2 m^3/hr. (8.8GPM).

4.7.4 Water pumps

The thermostatic water systems are driven by water pumps, selected as light horizontal multistage centrifugal pumps, which are manufactured by Southern Pump Company.

Figure 4-6. Photos of main instrument in water loop system

Top left, chilled water unit; Top right, water tank; Bottom left, electric boiler; Bottom right, cooling tower.

4.8 Equipment installation

We set our lab on the first floor of our laboratory building. Tap water and 220V/ 380V with 50 amperes maximum wire capacity are provided. An $8m^3$ ($275ft^3$) cubic foundation was built in the room for the installation of the vibration table in order to reduce the impacts on surrounding objects. After the vibration table was settled, the chiller was fixed on the vibration table. We used 30 pieces of 10 mm/0.4 inch screws to ensure the security of the vibration experiment. After that, we put all the platinum thermal sensors on the machine by drilling holes on the tubes with thermal conduction oil to ensure enough thermal transfer.

All the flow meters were connected with flange connection. Soft connection was used between the chiller and the thermostatic water loop system to greatly isolate the vibration. Similarly, the vacuum pump and chiller control panel were located outside of the absorption chiller to avoid resonance from vibration.

Chapter 5 Methodology and Data Analysis

The goal of this project is to study the heat and mass transfer difference of the absorption chiller with and without vibration. Thus, the heat and mass transfer calculation is very important to us. As we showed in the previous tables, we record all the temperatures, solution flow rates and solution concentrations in the system. The procedure of how to get heat and mass transfer in absorber is shown in the following sections.

5.1 Mass transfer analysis

In the experiment, the weak and strong concentration values were collected with the in-line concentration sensors, and the weak solution flowrate collected by the solution flow meter. We did not know the strong solution flow rate directly. However, based on the mass conservation of pure lithium-bromide (Li-Br) in the absorber in a steady-state, we could calculate the strong solution flowrate by using equation:

$$\dot{V}_{weak} * X_{weak} * \rho_{weak} = \dot{V}_{strong} * X_{strong} * \rho_{strong} \qquad (1)$$

Where,

X_{weak}, weak solution concentration;

X_{strong}, strong solution concentration;

$\dot{V}_{weak}$, weak solution flow rate;

$\dot{V}_{strong}$, strong solution flow rate;

ρ_{weak} , weak solution density, and

ρ_{strong} , strong solution density.

The density of lithium-bromide is defined by:

$$\rho = \sum_{0}^{3} A_n X^n + T \sum_{0}^{3} B_n X^n \qquad (2)$$

n	0	1	2	3
A_n	1016.028	884.165	-419.036	1696.176
B_n	-4.903	27.309	-55.465	36.273

X and *T* are the solution concentration and temperature of solution, respectively. This equation is used when the concentration of lithium-bromide is between 40%-66%, which is the case in our experiment.

Combing Eq. 1 and 2, we get,

$$\dot{V}_{strong} = \frac{\dot{V}_{weak} * X_{weak} * \rho_{weak}}{X_{strong} * \rho_{strong}} \qquad (3)$$

Since, in the steady-state, the mass of lithium-bromide remains constant in the absorber, the mass flow rate difference between the weak solution and the strong solution gives us the mass transfer rate from the water vapor into the solution, as:

$$\dot{m}_{water,ab} = \dot{V}_{weak} * \rho_{weak} - \dot{V}_{strong} * \rho_{strong} \qquad (4)$$

The mass transfer calculation process is illustrated in Fig.5-1. The variables in gray are directly measured from the sensors or calculated with empirical equations. The link

between the primary variables, derivative variables and the final results are illustrated with curves in different colors.

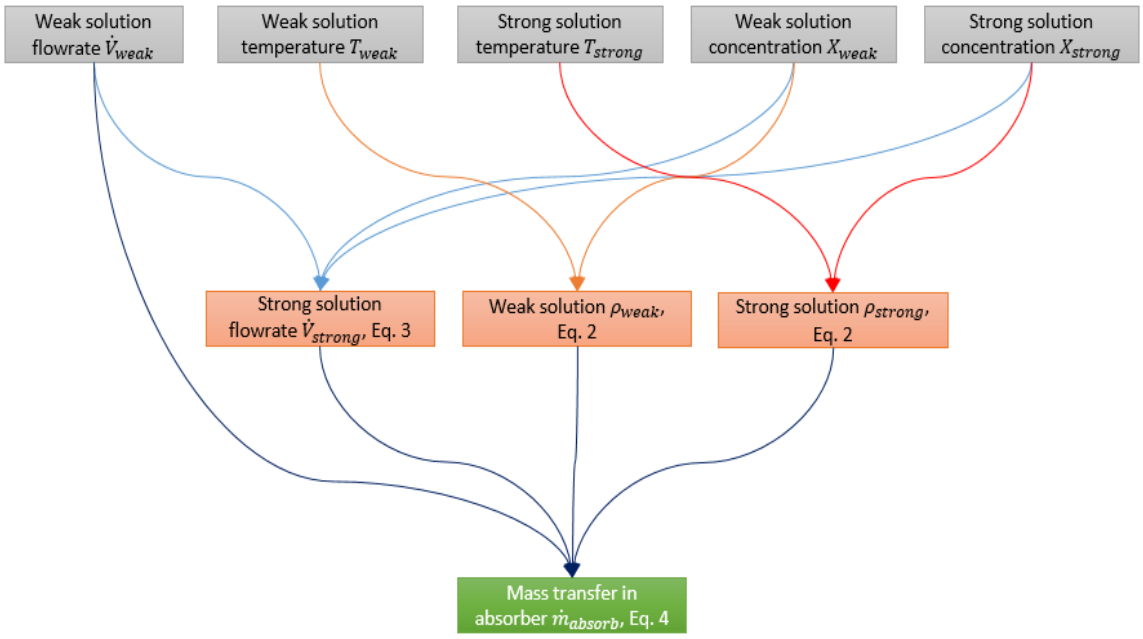

Figure 5-1. Calculation process for mass transfer

5.2 Heat transfer analysis

Heat transfer in the absorber observes the energy conservation law and can be calculated by using the following equation,

$$Q_{abs} = \dot{V}_{strong} * \rho_{strong} * h_{abs,in,sol} + \dot{m}_{water,ab} * h_{water,evp} - \dot{V}_{weak} * \rho_{weak} * h_{abs,out,sol} \quad (5)$$

Where,

$h_{abs,in,sol}$, enthalpy of inlet strong solution;

$h_{abs,out,sol}$, enthalpy of outlet weak solution;

(the enthalpy equation of the solution can be found in Lansing F. L, 1976)

$h_{water,evp}$, water vapor condensing heat during sorption process, which is a function of the mixture pressure or temperature when the vapor is considered saturated. The values can be directly obtained from the common thermal dynamic tables. Fig. 5-2 illustrates the calculation process for the heat transfer in the absorber.

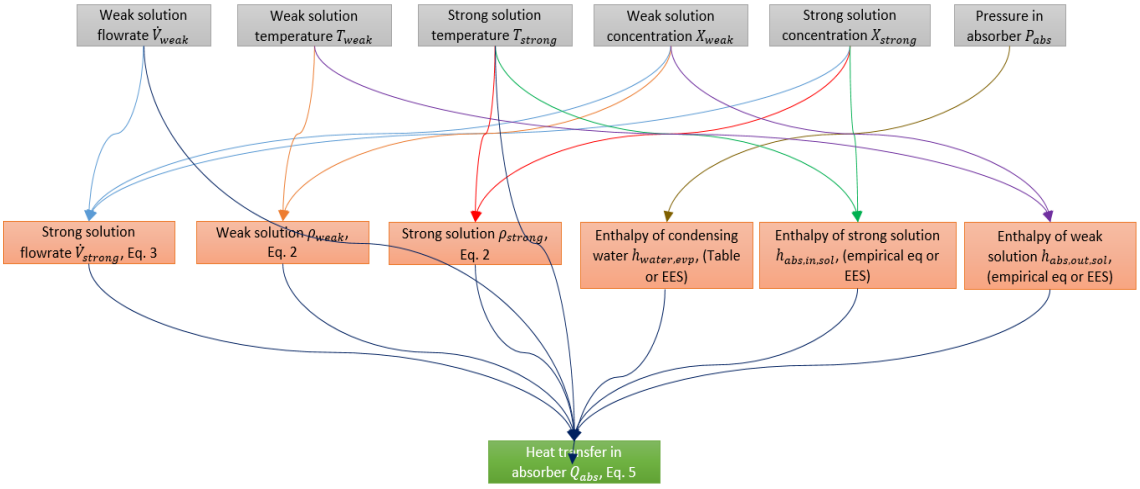

Figure 5-2. Calculation process for heat transfer

Chapter 6 Experiment plan introduction

There are several influence factors in the chiller when vibration is introduced to a lithium bromide absorber. The factors include vibration frequency, vibration amplitude, solution flow rate and additive.

Frequency is one of the most important elements of vibration. The frequency influences molecular activity, and high frequency may destroy the film layer boundary to let mass transfer happen easier. However high frequency also induces resonance and more energy cost. On the other hand, most of the parts in absorption chiller are metals, and some of them are very thin. The resonance frequency range of thin metal is close to our experiment. Thus, the selection of frequency range is very critical.

Amplitude is another important element during vibration. In falling film absorption chiller, vibration amplitude may provide inertia force to accelerate the liquid film falling and increase the contact area between film and vapor. It will also accelerate molecular activity. In the following parts, we will introduce the influence from different amplitude.

Solution flow rate is also an important element in our experiment, because different solution flow rate will induce different film thickness. Thickness is the most important physical property of falling film absorption cycle. So we conduct vibration experiment under different solution flow rates.

Additive is widely used in absorption chiller system. It provides about 15%-20% extra performance to the system. There are two kinds of additives frequently used, 2EH and n-

octanol. So we conduct vibration experiment under three conditions, with 2EH, with n-octanol and without additive.

We separated the experiment into different sub-categories to test the impacts by each factor while the related parameters were maintained in a range and conditions as shown in Table 6-1.

Cooling water inlet temperature	28-30^{o}C (82.4-86^{o}F)
Hot water inlet temperature	90-95^{o}C (194-203^{o}F)
Chilled water inlet temperature	10-15^{o}C (50-59^{o}F)
Chilled water outlet temperature	7.5-13^{o}C (45.5-55.4^{o}F)
Evaporating temperature	6-11.5^{o}C (42.8-52.7^{o}F)
Strong solution concentration range	60%-63%
Weak solution concentration range	58%-60.5%
2EH additive concentration	500 ppm

Table 6-1: Operating conditions of the absorption chiller in this research project

Chapter 7 Experiment result and analysis

7.1 Short-term tests

At the first phase of this project, we conducted a lot of preliminary tests with short-term vibration experiments from Fall 2013 to Spring 2014. The short-term vibration tests explored the most suitable range of vibration frequency and amplitude that do not result in resonance. During this period, we also fine-tuned the water-loop control strategies and did troubleshooting of errors that we found in the sensor acquisition system during those tests. Sensor uncertainty analyses were also conducted during the process.

Although most absorption chillers in the market use the 2EH additive, the chiller used in this project was shipped with the n-octanol additive. Thus, we conducted these preliminary tests with the n-octanol additive. Most of the results were obtained with vibration in 20-30 minutes, thus the chiller may not have reached steady state yet. At that time, the in-line concentration sensors were not installed to the chiller, thus we could only calculate the cooling performance from the chilled water temperature difference and the chilled water flowrate.

These experimental frequencies were from 5Hz to 100Hz, the amplitudes were from 0.05 to 1mm (0.002 to 0.039inch), and the solution flow rates were from 0.1 to 0.5m^3/h (0.44-2.2GPM). With n-octanol additive, under frequency under 10 Hz, the enhancement was not quite noticeable. For frequencies from 15 Hz to 30 Hz, we found more consistent and noticeable enhancement at the cooling capacity (up to 20%). For a higher frequency at 55 Hz to 80 Hz, the data were less consistent and the enhancements were at a smaller range.

Besides, vibration at higher frequency will require much more energy and will have higher risk of equipment damage. Therefore, we did not include these frequency ranges in the long-term tests. Regarding the amplitude, we found 0.15-0.25mm (0.0059-0.0098inch) has the most positive enhancement. For different solution flowrates, 0.2-0.3m^3/h (0.88-1.32GPM) always presented more significant enhancement when comparing to other solution flowrates.

Experiment Condition			Experiment Result		
Frequency	Amplitude mm	Solution Flow Rate m^3/h	Positive Effect %	No noticeable effect	Negative Effect
5Hz	0.5	0.2			√
	0.8			√	
8Hz	0.8		6%		
10Hz	0.15	0.3	6%		
	0.25	0.3		√	
	0.4	0.2		√	
	0.5	0.2		√	
	0.8	0.2			√
12Hz	0.8	0.2	12.5%		
14Hz	0.8	0.2	10%		
15Hz	0.25	0.3	5%		
	0.4	0.2	23%		
25Hz	0.1	0.3	5.5%		
	0.15	0.2	8%		
	0.2	0.3	11%		
	0.25	0.3	9%		
	0.3	0.3	5.5%		
	0.35	0.3	6%		
	0.4	0.3	5.4%		
50Hz	0.15	0.2			√
	0.2	0.2			√
55Hz	0.15	0.3			√
60Hz	0.1	0.2	11%		
	0.13	0.2	5%		
	0.15	0.3		√	

65Hz	0.15	0.2			
75Hz	0.1	0.3	3%		
80Hz	0.1	0.2	7.7%		
	0.18	0.2	3.5%		
100Hz	0.1	0.2		√	
	0.164	0.2	7.4%		
20Hz,30Hz,35Hz,40Hz,45Hz resonance					

Table 7-1: short-term experiment result

NOTE: Positive effect experiment vibration conduct between 30 minutes to 60 minutes, we stopped the vibration when we couldn't observe any change after 20 minutes. No effect vibration experiment conduct vibration 30 minutes. Negative experiment conduct vibration 20 to 30 minutes.

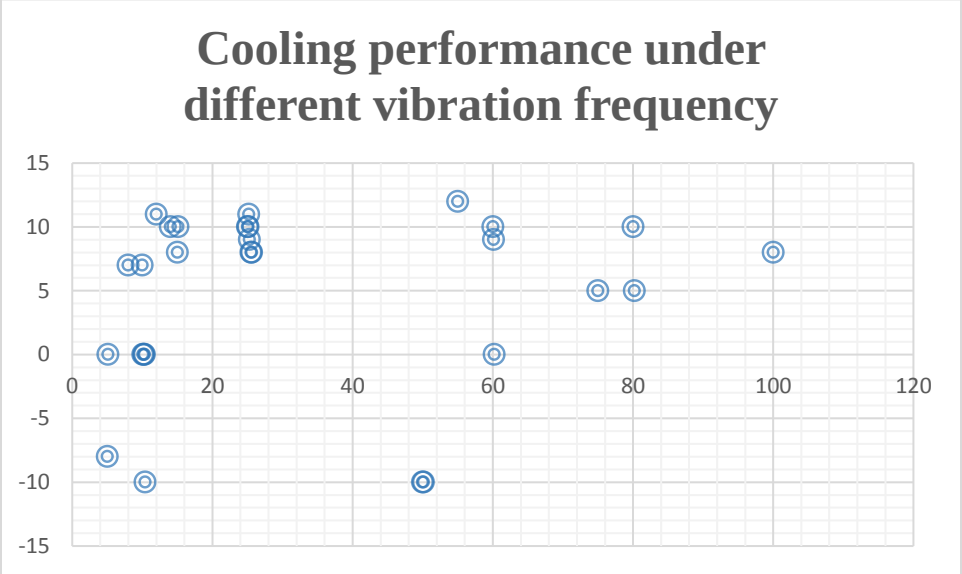

Figure 7-1: Cooling performance under different vibration frequency

From this figure, we could observe most of the enhancement happened from 15Hz to 25Hz. Within this frequency range, the enhancement is most stable. In the range of 0-15Hz. The vibration effect is unpredictable. Under high frequency range, 60Hz -100Hz, most of the performance is also positive, the percentage of increased performance is very likely as

under 15-25Hz. However, high frequency introduces more resonance and more energy cost. Thus, we do not recommend high frequency vibration.

For different amplitude, we could not define any conclusion. The test amplitude mostly from 0.1mm to 0.35mm. There is not obvious amplitude effect from this experiment. From energy consumption concern, we recommend use the amplitude from 0.1mm to 0.25mm to save energy. And more amplitude experiments were conducted in the further experiment under the conditions with 2EH additive and without additive.

Therefore, when we planned for the experiment with 2EH additive, we also targeted at 15Hz to 30Hz (resonance frequency at 35Hz to 55 Hz). The results with n-octanol additive do not provide us the solution concentration information for the absorber heat and mass transfer analysis and it is not intended to be compared directly to the results from the long-term tests.

7.2 Long-term tests

After half a year preliminary experiment, the long term test started based on the results of short term tests. For the frequency, we focus on 15Hz to 30Hz and for the amplitude we focus on 0.1mm to 0.4mm. Considering that additives may impact the effect of mechanism motions on the absorber, this part of test is separated into the test without additive (7.2.1-7.2.4) and the test with 2EH additive (7.2.5-7.2.7). The long-term vibration experiment plan was set up as the following groups based on the short-term test experience.

From the preliminary experiments, we found different solution flowrates have different enhancement when a vibration was introduced. Considering different solution flowrates result in different film thickness on the tube surface in the absorber, it is

reasonable to assume that, when a vibration is introduced, we will have different heat and mass transfer enhancement in the system with different solution flowrates. We conducted the experiments to test the influences of different solution flow rate from 0.1-0.5 m^3/h (0.44-2.2 GPM) under fixed vibration combination 25Hz, 0.2mm/0.79inch, which is shown in 7.2.1 and 7.2.5 for the case without and with an additive.

Amplitude is one of the most important controlled variables in this test. From the preliminary experiments, we knew the optimal amplitude is from 0.15-0.25 mm/0.59-0.98 inch. Thus we extended the test range a little bit, and conducted the long term experiment from 0.1mm-0.4 mm/0.39-1.57 inch under fixed amplitude 25Hz and 15Hz. The result is shown in 7.2.2, 7.2.3 and 7.2.6. The reason we test both 15Hz and 25Hz is to separate the frequency effect from other aspects.

Frequency is another important variable for vibration tests. From the preliminary experiments, we found the most optimal frequency is from 20-30Hz. Thus we conducted the long term experiments from 15-30Hz frequency under the fixed amplitude 0.2mm, which is shown in 7.2.4 and 7.2.7.

In this section, we mainly compare seven sets of results in the long-term tests as grouped in Table 7-2.

Experiments without additive (7.2.1-7.2.4)		**Controlled variables**	**Purpose**
Set 1. (7.2.1)	Different solution flow rate tests with a fixed vibration condition at 25Hz, 0.2mm	Solution flow rate: $0.1m^3/h$ - $0.5m^3/h$; 0.44GPM-2.2GPM	Find out effect from different solution flow rates
Set 2. (7.2.2)	Different amplitude tests with fixed frequency 25Hz	Amplitude: 0.1mm-0.4mm (0.39inch-1.57inch)	Find out effect from different vibration amplitudes

Set 3. (7.2.3)	Different amplitude tests with a fixed frequency at 15Hz	Amplitude: 0.1mm-0.4mm (0.39inch-1.57inch)	Find out effect from different vibration amplitudes, compare the results with 15Hz to that with 25Hz
Set 4. (7.2.4)	Different Frequency tests with a fixed amplitude at 0.2mm	Frequency: 15Hz-30Hz	Find out effect from different vibration frequencies
Experiments with 2EH additive (7.2.5-7.2.7)		**Controlled variables**	**Purpose**
Set 5. (7.2.5)	Different solution flow rate tests with a fixed vibration condition at 25Hz, 0.2mm	Solution flow rate: $0.1m^3/h$ - $0.4m^3/h$ (0.44GPM-1.76GPM)	Find out effect from different solution flow rate
Set 6. (7.2.6)	Different amplitude tests with a fixed frequency at 25Hz	Amplitude: 0.1mm-0.4mm (0.39inch-1.57inch)	Find out effect from different vibration amplitudes
Set 7. (7.2.7)	Different Frequency tests with a fixed amplitude at 0.2mm	Frequency: 15Hz-30Hz	Find out effect from different vibration frequencies

Table 7-2: Summary of experiment sets

Summarized results for the controlled tests in Table 7-2 are shown in the following tables and figures.

Detailed results are collected in the appendix of this report. In each table, we provide the vibration frequency and amplitude. The varied parameters are highlighted in light blue. Film thickness, amplitude to thickness ratio, enhancement percentage and vibration duration are listed. Under each table, we use column charts to illustrate the percentage of enhancement without and with vibration.

7.2.1 Different solution flow rate enhancement (Without additive)

Freq. (Hz)	Amplitude		Solution flow rate		Film thickness		Amplitude to thickness ratio (%)	Enhancement (%)		Vibration Duration (minutes)
	Inch (10^{-2})	mm	GPM	m^3/h	Inch (10^{-2})	mm		Mass transfer	Heat transfer	
25	0.79	0.2	0.44	0.1	1.73	0.44	45	0	0	45
25	0.79	0.2	0.88	0.2	2.2	0.56	36	38	41.8	50
25	0.79	0.2	1.32	0.3	2.5	0.64	31	34.3	31.7	50
25	0.79	0.2	1.76	0.4	2.8	0.7	29	15.6	16.8	60
25	0.79	0.2	2.2	0.5	3	0.76	26	4	4	55

Table 7-3: Experiment parameters settings and results under 25Hz, 0.2mm/0.0079inch vibration

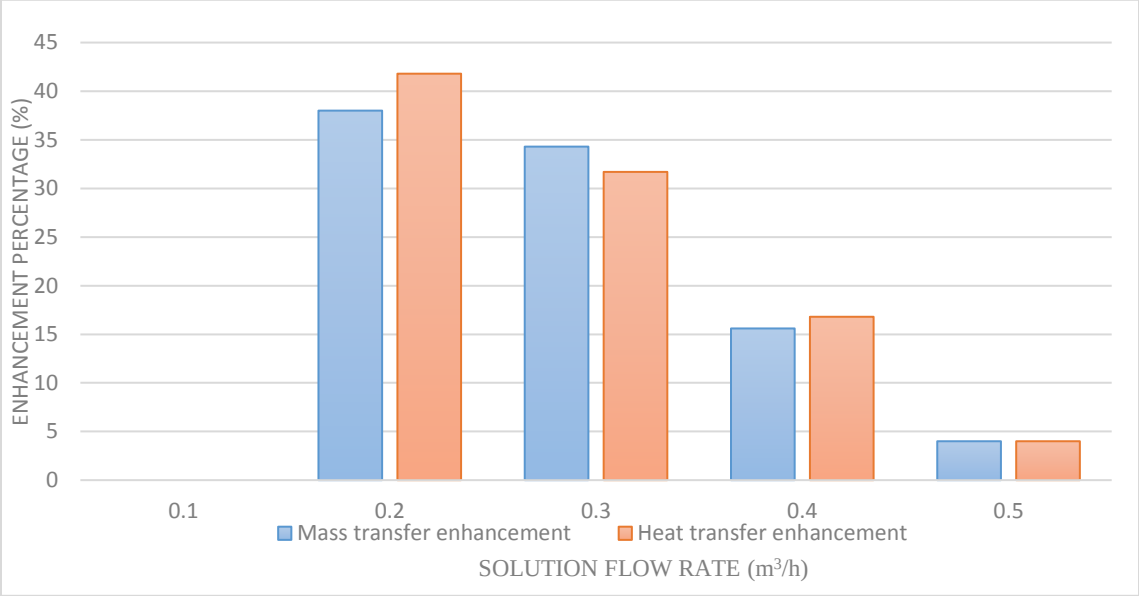

Figure 7-2. Heat and mass transfer enhancement with different solution flow rates (fixed condition 25Hz, 0.2 mm/0.0079 inch, without additive)

From this figure, we can observe that with different solution flowrates (i.e. film thickness,), heat and mass transfer have different improvement from the same vibration condition. Under relatively high flowrate (i.e. 0.5 m^3/h (2.2 GPM)) and low solution flowrate (i.e. 0.1 m^3/h (0.44 GPM)), there is barely heat and mass transfer enhancement in the absorber. Under medium range 0.2-0.4 m^3/h (0.88-1.76 GPM) solution flowrate, there

are significant heat and mass transfer enhancement, especially under 0.2-0.3 m^3/h (0.88-1.32 GPM) condition. The higher solution flowrate means higher solution spray density, which also causes the film thickness in the tubes to be thicker. The detail experiment parameters are shown in Appendix C.1.

The solution film thicknesses were calculated from the equation by Jayasekara and Halgamuge (2013).

$$\delta = \left[\frac{3\mu\Gamma}{(\rho_l - \rho_v)^2 g sin\theta}\right]^{\frac{1}{3}} \qquad (1)$$

Where,

Γ, Liquid mass flow rate pass unit width.

μ, Lithium Bromide solution dynamic viscosity (Source: Wang K., Abdelaziz and Vineyard E. A, 2012)

ρ_l, Lithium Bromide density

ρ_v, Vapor density under absorption pressure

g, gravitational acceleration

θ, film thickness allocation angle from vertical direction

The film thickness is different under different solution flow rate, and the detail film thickness is shown in the following sheet.

Solution flow rate (m^3/h)	0.1	0.2	0.3	0.4	0.5
Film thickness (mm)	0.17	0.20	0.25	0.29	0.33

7.2.2 Different amplitude enhancement (25Hz) (Without additive)

Freq. (Hz)	Amplitude		Solution flow rate		Film thickness		Amplitude to thickness ratio (%)	Enhancement (%)		Duration of the vibration (minutes)
	Inch (10^{-2})	mm	GPM	m^3/h	Inch (10^{-2})	mm		Mass transfer	Heat transfer	
25	0.39	0.1	0.88	0.2	2.2	0.56	18	0	0	70
25	0.79	0.2	0.88	0.2	2.2	0.56	36	38	41.8	50
25	1.18	0.3	0.88	0.2	2.2	0.56	54	18	17.5	70
25	1.57	0.4	0.88	0.2	2.2	0.56	72	15.8	11.4	60

Table 7-4: Experiment parameters settings and results under 25Hz, 0.2 m^3/h (0.88 GPM)

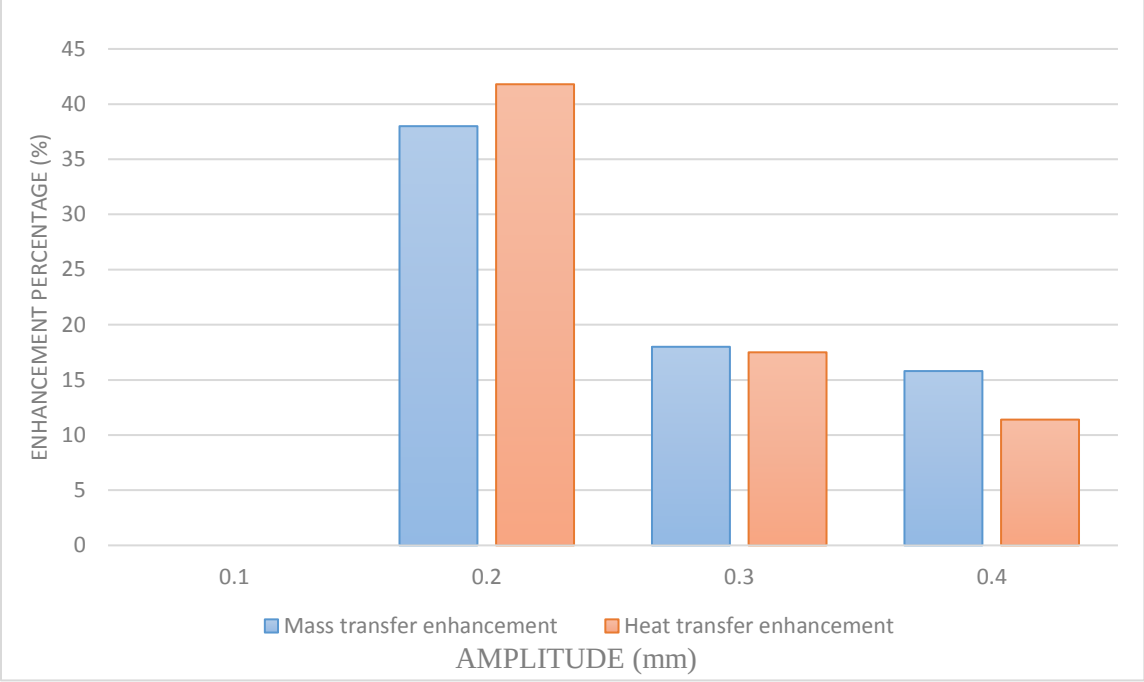

Figure 7-3. Heat and mass transfer with different amplitudes (fixed condition 25Hz 0.2 m^3/h (0.88 GPM))

In this group of data, we could observe during very low amplitude, there is basically no enhancement (or very little). It seems such tiny vibration could not induce film surface

change and vortex in the film. When the amplitude reaches 0.2 mm/0.0079 inch, the result shows very positive data from the vibration. The effect continues from 0.2 mm/0.0079 inch to 0.4 mm/0.1157 inch. Consider higher amplitude consuming more energy but no better enhancement, 0.2 mm/0.0079 inch is the most optimal amplitude in our test. The detail experiment parameters are shown in Appendix C.2.

In short term experiment, 0.2 mm has only about 15% enhancement. There are several reasons that may introduce the enhancement difference. The first one is the experiment time. Short term experiment only has 20-30 mins' vibration, and the enhancement may not reach the maximum yet. The other reason may be from the additive. The additive and vibration effect may have some overlap. The function of additive is to enhance molecular activity and break the surface tension of film. This is similar as the vibration function. We will also compare with the experiment with 2EH additive later to get more confident conclusion.

7.2.3 Different amplitude enhancement (15Hz) (Without additive)

Freq. (Hz)	Amplitude		Solution flow rate		Film thickness		Amplitude to thickness ratio (%)	Enhancement (%)		Duration of the vibration (minutes)
	Inch (10^{-2})	mm	GPM	m^3/h	Inch (10^{-2})	mm		Mass transfer	Heat transfer	
15	0.59	0.15	0.88	0.2	2.2	0.56	27	6	5	60
15	0.79	0.2	1.32	0.3	2.5	0.64	31	7.4	6.9	45
15	0.98	0.25	0.88	0.2	2.2	0.56	45	6.7	7	40
15	1.18	0.3	1.32	0.3	2.5	0.64	47	2	1	40
15	1.38	0.35	0.88	0.2	2.2	0.56	63	2	2	50

Table 7-5: Experiment parameters settings and results under 15 Hz vibration

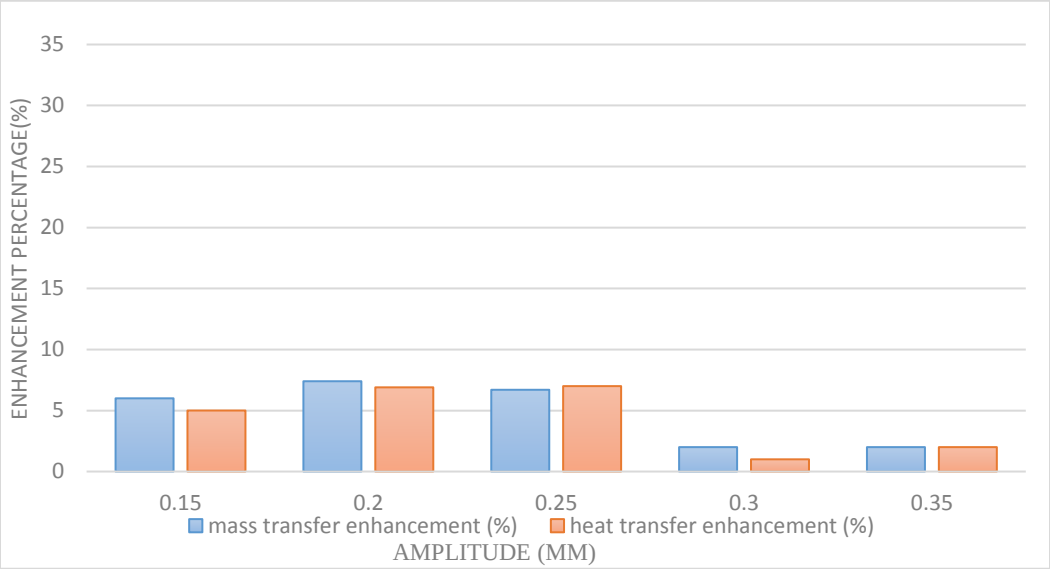

Figure 7-4. Heat and mass transfer with different amplitudes (fixed condition 15Hz, 0.2-0.3 m^3/h (0.88-1.32 GPM))

This group of experiment is under different amplitude with 15Hz frequency. In this group of tests, amplitudes 0.2 mm/ 0.0079 inch and 0.25 mm/ 0.0098 inch have the best performance enhancement. However, the enhancement is not big, only less than 10% as shown in the figure.

From this group of experiments, we could observe the critical amplitude point is likely at 0.25 mm. After the amplitude reaches 0.3 mm, the performance enhancement reduces to only 20%

7.2.4 Different frequency enhancement (Without additive)

Freq(Hz)	Amplitude		Solution flow rate		Film thickness		Amplitude to thickness ratio (%)	Enhancement (%)		Duration of the vibration (minutes)
	Inch (10^{-2})	mm	GPM	m^3/h	Inch (10^{-2})	mm		Mass transfer	Heat transfer	
15	0.79	0.2	1.32	0.3	2.5	0.64	31	4.5	4	50
20	0.79	0.2	1.32	0.3	2.5	0.64	31	10.6	8.5	70
25	0.79	0.2	1.32	0.3	2.5	0.64	31	34.3	31.7	50
30	0.79	0.2	1.32	0.3	2.5	0.64	31	10.7	8.7	35

Table 7-6: Experiment parameter settings and results under 0.2mm, 0.3m^3/h (1.32GPM)

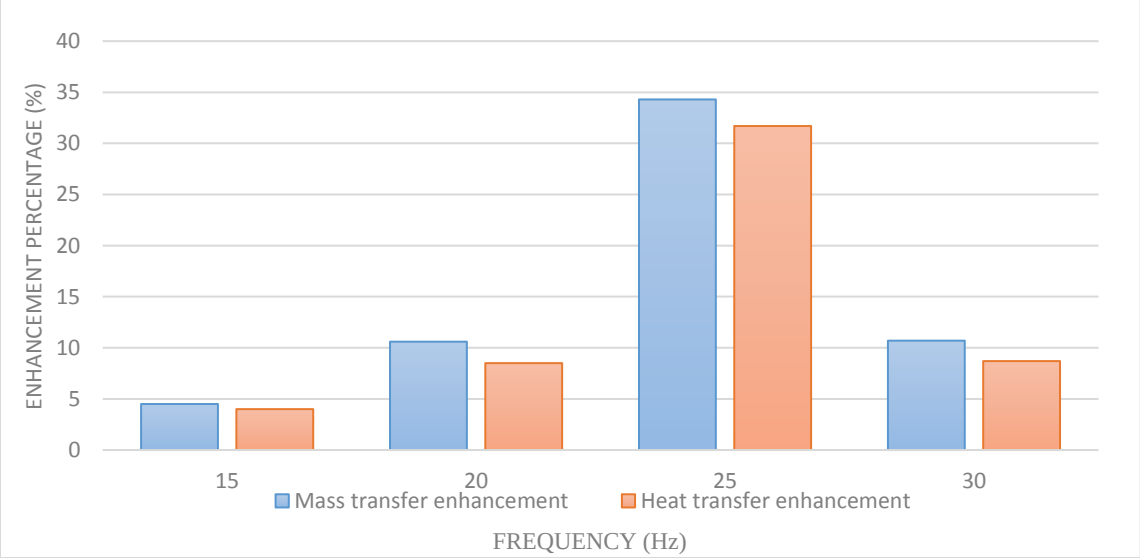

Figure 7-5. Heat and mass transfer with different frequency (fixed condition 0.2 mm (0.0079 inch) 0.3 m^3/h (1.32 GPM))

From this group of data, we can observe that there are different influences under different frequencies to the heat and mass transfer in the absorber. 25Hz has much better enhancement among the test, which doubles the enhancement from 20Hz and 30Hz and triples from 15Hz. Thus for this particular type of absorption chiller, 25 Hz frequency

might be used to improve the performance. Compared to 15Hz test group in the last section, 25Hz has better enhancement under all conditions. The detailed experiment parameters are shown in Appendix C.3.

7.2.5 Different solution flow rate enhancement (With 2EH additive)

Freq. (Hz)	Amplitude		Solution flow rate		Film thickness		Amplitude to thickness ratio (%)	Enhancement (%)		Duration of the vibration (minutes)
	Inch (10^{-2})	mm	GPM	m^3/h	Inch (10^{-2})	mm		Mass transfer	Heat transfer	
25	0.79	0.2	0.44	0.1	1.73	0.44	45	7.4	8.7	50
25	0.79	0.2	0.88	0.2	2.2	0.56	36	28.7	34	50
25	0.79	0.2	1.32	0.3	2.5	0.64	31	21.5	17.8	42
25	0.79	0.2	1.76	0.4	2.8	0.7	29	16.7	19.8	60

Table 7-7: Experiment parameters settings and results under 25Hz, 0.2mm/0.0079inch vibration

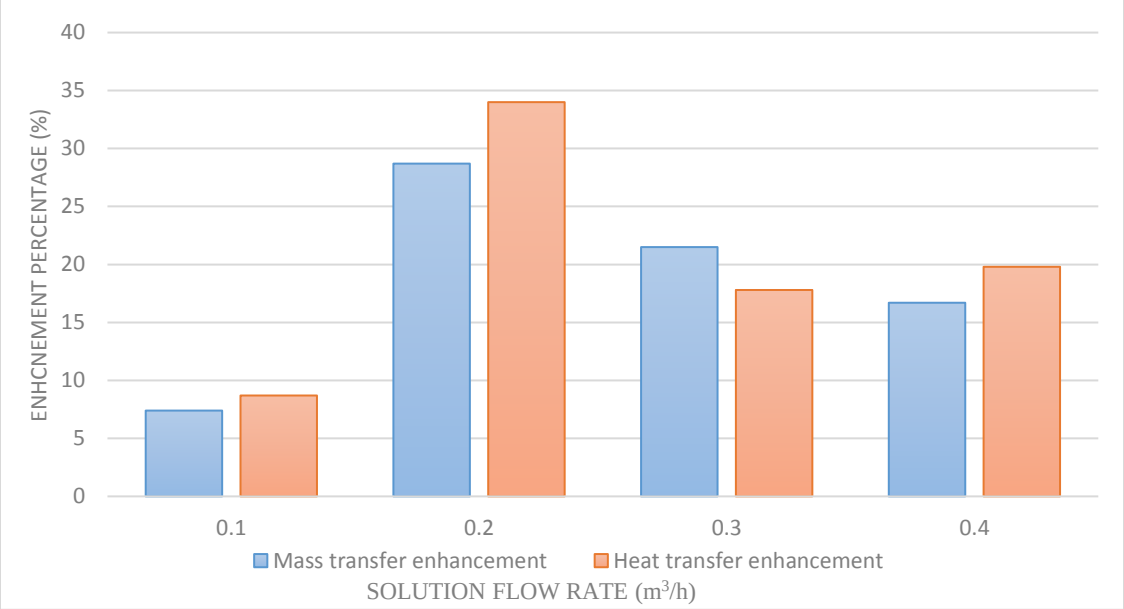

Figure 7-6. Heat and mass transfer with different solution flow rates (fixed condition 25 Hz, 0.2 mm/0.0079 in)

After adding 2EH additive, we observed that different solution flow rates also have some kind of influence on the absorber, under same vibration condition. However,

compared to the experiment without additive, the enhancement difference is much smaller. For 0.2-0.4 m^3/h (0.88-1.6 GPM) solution flow rate, the enhancement from different solution flowrates is very similar. For 0.1 m^3/h (0.22 GPM) solution flow rate, the result with additive has an improved enhancement (20% compare to 1%). The detailed experiment parameters are shown in Appendix C.4.

Compared to group 1 (different solution flow rate without additive), the trend is generally the same. The performance peak happens under 0.2 m^3/h solution flow rate (0.2 mm film thickness). The thickness is the same as vibration amplitude. We have a hypothesis that the vibration enhanced performance is bigger when the film thickness is similar as the vibration amplitude. However, this hypostasis still need further experiments to testify and the theory of this phenomenon still remains unavailable.

7.2.6 Different amplitude enhancement (With 2EH additive)

Freq. (Hz)	Amplitude		Solution flow rate		Film thickness		Amplitude to thickness ratio (%)	Enhancement (%)		Duration of the vibration (minutes)
	Inch (10^{-2})	mm	GPM	m^3/h	Inch (10^{-2})	mm		Mass transfer	Heat transfer	
25	0.39	0.1	0.88	0.2	2.2	0.56	18	16.6	18.7	45
25	0.79	0.2	0.88	0.2	2.2	0.56	36	28.7	34	50
25	1.18	0.3	0.88	0.2	2.2	0.56	54	27.8	29.4	45
25	1.57	0.4	0.88	0.2	2.2	0.56	72	12.6	14	60

Table 7-8: Experiment parameters settings and results under 25 Hz, 0.2 m^3/h (0.88 GPM)

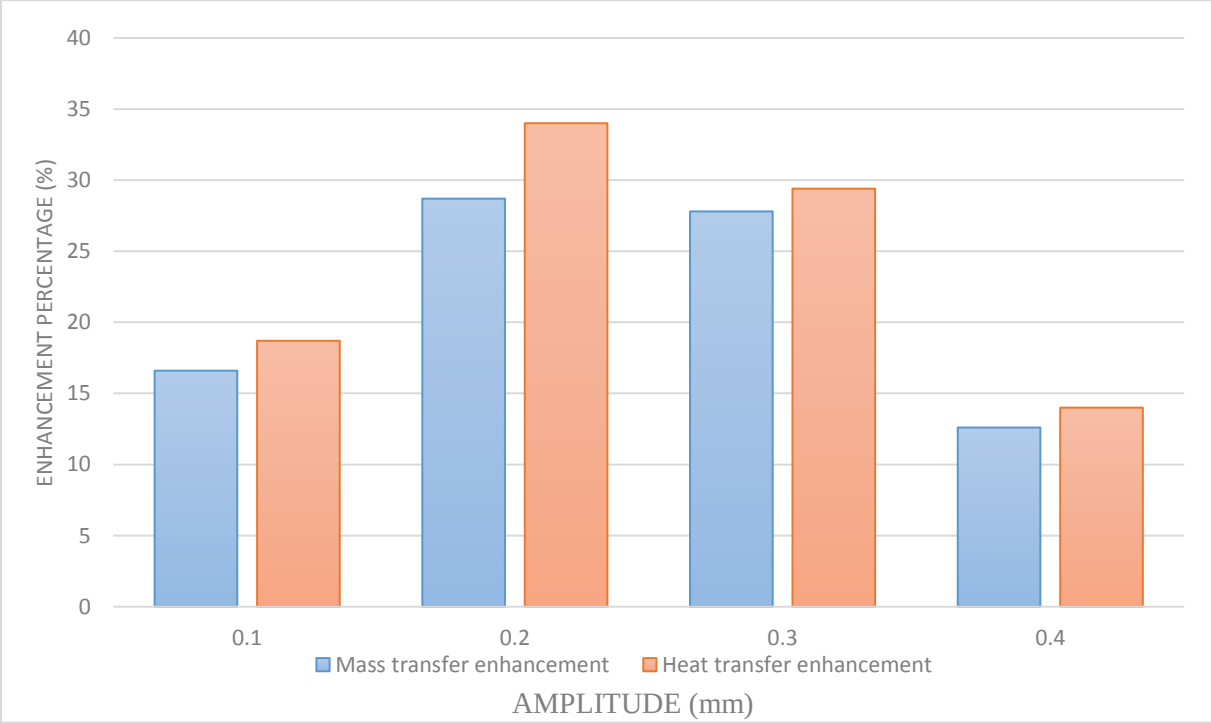

Figure 3-7. Heat and mass transfer enhancement with different amplitudes. (fixed condition 25 Hz, 0.2 m^3/h (0.88 GPM))

Compared to the data without additive, we observe 0.2 mm/0.0079 inch and 0.3 mm/0.0118 inch amplitude conditions also have the highest enhancement from vibration. The difference also exists under 0.1 mm/0.0039 inch vibration condition; the enhancement

with additive reaches 18%. Meanwhile there is barely any enhancement without additive. The detailed experiment parameters are shown in Appendix C.5.

Compared to group 2 (different amplitude without additive) we could observe the trend is also very similar. 0.2 mm amplitude has the best performance from vibration effect.

7.2.7 Different frequency enhancement (With 2EH additive)

Freq. (Hz)	Amplitude		Solution flow rate		Film thickness		Amplitude to thickness ratio (%)	Enhancement (%)		Duration of the vibration (minutes)
	Inch (10^{-2})	mm	GPM	m^3/h	Inch (10^{-2})	mm		Mass transfer	Heat transfer	
15	0.79	0.2	1.32	0.3	2.5	0.64	31	9	9.9	50
20	0.79	0.2	1.32	0.3	2.5	0.64	31	22.2	22	40
25	0.79	0.2	1.32	0.3	2.5	0.64	31	24.8	27.4	45
30	0.79	0.2	1.32	0.3	2.5	0.64	31	19.4	21.1	100

Table 7-9: experiment parameters settings and results under 0.2mm, 0.3m^3/h (1.32GPM)

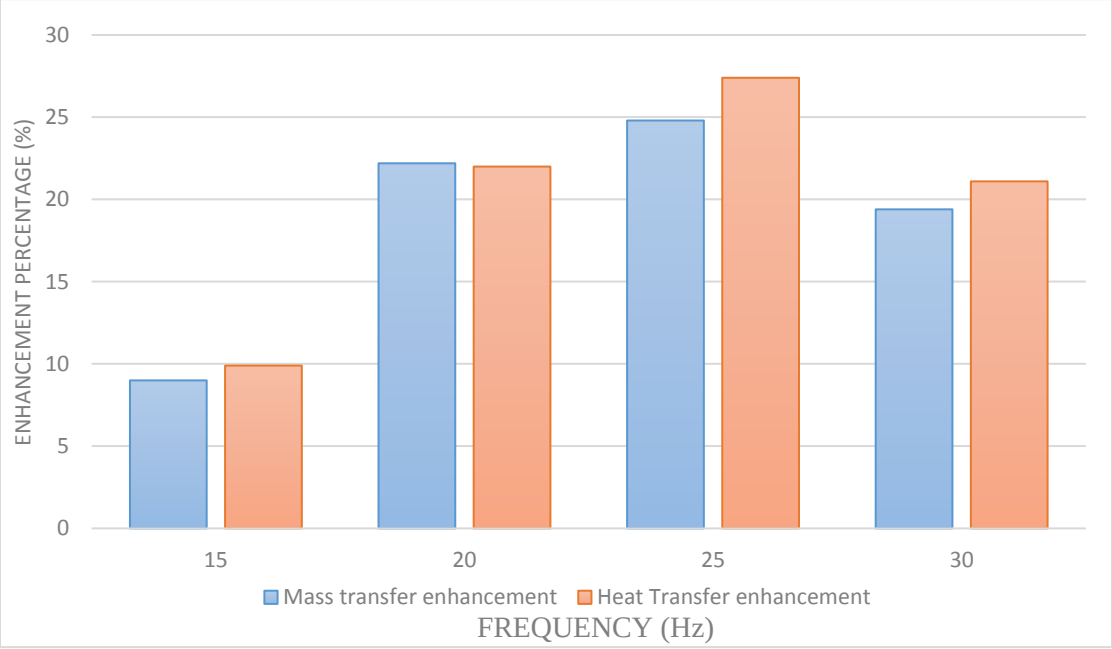

Figure 7-8. Heat and mass transfer enhancement with different frequencies. (fixed condition 0.2mm, 0.3m^3/h (1.32GPM))

From this group of data, we also observe 25Hz has the highest enhancement, which is the same result as without additive, and the enhancement amount is also similar. The differences from the enhancement margin under 15Hz, 20Hz and 30Hz are shown in the figure. The enhancement with additive is a little bit bigger in these three conditions. The detail experiment parameters are shown in Appendix C.6.

Compared to group 4 (different frequency performance without additive), the peak performance frequency is also happening under 25Hz. However, the 20Hz and 30Hz conditions have some difference. During the experiment with additive, both 20Hz and 30Hz have performance enhancement better than 20%. In the experiment without the additive, 20Hz and 30Hz only have 10% enhancement. This phenomenon possibly plays some of the role of vibration effect. Thus makes the critical peak frequency range bigger compare without additive. This phenomenon could be only testified with more experiment and more scientific theory analysis.

Chapter 8 Summary and discussions

In this project, we reviewed the literature on the effects of mechanisms on the heat and mass transfer in the absorption process, designed and constructed an active mechanism for enhancing the heat and mass transfer, and evaluated the heat and mass transfer performance when the mechanism was introduced to the chiller. Experiments were conducted to identify the effects of vibration frequency and amplitude on the absorber performance. Other factors, including the flowrates and additive, that could impact the effects were also investigated. The test results were presented in this thesis.

Based on the results for the commercial chiller used in this study, we can draw the following conclusion:

The vibration mechanism on the chiller can impact the heat and mass transfer process in the absorber; therefore, it might be applicable by commercial manufacturers as a technology to improve the performance of absorption chillers;

There is an optimal combination of vibration frequency and amplitude that can best enhance the heat and mass transfer for a specific chiller and configuration. For this chiller, the optimal conditions are 25 Hz and 0.2-0.3 mm. Without additive, there is nearly 40% enhancement at the optimal conditions. With 2EH additive, the enhancement is still nearly 30-35%. While there are also impacts from other vibration combinations, they seem to be less effective compared to the optimal set;

The presence of the additive changes the final performance of the heat and mass transfer in the absorber, when the vibration is introduced, in terms of the enhancement percentage among the combinations;

There are also some extra findings from our experiments. Such as the amplitude's impact on the performance is better when it is close to the film thickness. And the additive enlarges the peak critical range compared with the condition without additive. However, these findings are not very confidential at this stage; more experiment and theory analysis should be done to testify them.

The heat and mass transfer inside of the absorber is a complicated and coupled process. There are many factors that might impact the performance, including the solution flowrates, working condition of the components, etc. Based on our experimental results, we observe positive impacts, more or less, on the heat and mass transfer process when a vibration is introduced. Although we don't have theoretical proof and/or microscopic measurements on the falling film, we speculate that the enhancement from the vibration is caused by the changed thickness and distribution between the unsaturated layer and saturated layer of the falling film. Future study is needed to fill the technical gap.

Chapter 9 Future study

From the theory aspect, the vibration effect in micro scope hasn't been studied. Using high speed camera could assist us to study the mechanism motion in micro scope. The images from a high speed camera could allow us directly observe the circumstance on the film surface. The findings could help us build a physical model of mechanism motion effect falling film surface.

The additive function is still not so clear under mechanism motion. Even without mechanism motion, the additive function is not very well-recognized in the world. Working on additive effect on theoretical level is one direction for absorption system. On the other hand, the functions of mechanism motion and additive have some overlap. If mechanism motion could enhance additive performance, it will also have the potential using in chemical engineering area.

For the absorption chiller industry, introducing vibration table to each chiller is not practical. It should seek some mechanism devices to introduce simpler mechanism motion. Such as vibrating only tubes buddle in absorber or using solution pulse pushing platform which linked with tubes buddle to provide specific vibration combination (such as 25Hz, 0.2mm).

References

Aoune, A. and C. Ramshaw. 1999. Process intensification: heat and mass transfer characteristics of liquid films on rotating discs. *International journal of heat and mass transfer*, 42(14):2543-2556.

Arun, M. B., M. P. Maiya and S. S. Murthy. 2000. Equilibrium low pressure generator temperatures for double-effect series fow absorption refrigeration systems. *Applied Thermal Engineering*, 20(3):227-242.

ASHRAE. 2010. 2010 ASHRAE Handbook. Atlanta, USA: American Society of Heating, *Refrigerating and Air-Conditioning Engineers*, Inc.

Babadi, F. and B. Farhanieh. 2005. Characteristics of heat and mass transfer in vapor absorption of falling film flow on a horizontal tube. *International Communications in Heat and Mass Transfer*, 32(9):1253-1265.

Barrera, M. A., R. Best, V. H. Gomez, O. G. Valladares, N. Velazquez and J. Chan. 2012. Analysis of the performance of a GAX hybrid (Solar-LPG) absorption refrigeration system operating with temperatures from solar heating sources. *Energy Procedia*, 30(-):884-892.

Bergles, A. E. and R. M. Manglik. 2013. Current progress and new developments in enhanced heat and mass transfer. *Journal of Enhanced Heat Transfer*, 20(1):1-15.

Bredow, D., P. Jain, A. Wohlfeil and F. Ziegler. 2008. Heat and mass transfer characteristics of a horizontal tube absorber in a semi-commercial absorption chiller. *Internationl Journal of Refrigeration*, 31(7):1273-1281.

Chen, R. H., Y. J. Lin and C. M. Lai. 2013. The Influence of Horizontal Longitudinal Vibrations and the Condensation Section Temperature on the Heat Transfer Performance of a Heat Pipe. *Heat Transfer Engineering*, 34(1):45-53.

Cheng, L., T. Luan, W. Du and M. Xu. 2009. Heat transfer enhancement by flow-induced vibration in heat exchangers. *International Journal of Heat and Mass Transfer*, 52(3):1053-1057.

Garimella, S., R. N. Christensen and D. Lacy. 1996. Performance evaluation of a generator-absorber heat-exchange heat pump. *Applied Thermal Engineering*, 16(7):591-604.

Garousi Farshi, L., S. M. S. Mahmoudi, M. A. Rosen, M. Yari and M. Amidpour. 2013. Exergoeconomic analysis of double effect absorption refrigeration systems. *Energy Conversion and Management*, 65(-):13-25.

Gomri, R. 2010. Investigation of the potential of application of single effect and multiple effect absorption cooling systems. *Energy Conversion and Management*, 51(8):1629-1636.

Harkins, W. D. 1952. The physical chemistry of surface films. New York: Reinhold.

Hoffmann, L., I. Greiter, A. Wagner, V. Weiss and G. Alefeld. 1996. Experimental investigation of heat transfer in a horizontal tube falling film absorber with aqueous solutions of LiBr with and without surfactants. *International Journal of Refrigeration*, 19(5):331-341.

Islam, M. R. 2008. Absorption process of a falling film on a tubular absorber:An experimental and numerical study. *Applied Thermal Engineering*, 28(11):1386-1394.

Jeong, S. and S. Garimella. 2002. Falling-film and droplet mode heat and mass transfer in a horizontal tube LiBr/water absorber. *International Journal of Heat and Mass Transfer*, 45(7):1445-1458.

Jun, Y. D., K. J. Kim and J. M. Kennedy. 2010. Dynamic surface tension of heat transfer additives suitable for use in steam condensers and absorbers. *Internationl Journal of Refrigeration*, 33(2):428-434.

Kiani, H., D. W. Sun and Z. Zhang. 2012. The effect of ultrasound irradiation on the convective heat transfer rate during immersion cooling of a stationary sphere. *Ultrasonics Sonochemistry*, 19(6):1238-1245.

Kim, J. S., H. Lee and S. I. Yu. 1999. Absorption of water vapour into lithium bromide-based solutions with additives using a simple stagnant pool absorber. *International Journal of Refrigeration*, 22(3) 188-193.

Kim, K. J., N. S. Berman, D. S. C. Chau and B. D. Wood. 1995. Absorption of water vapour into falling films of aqueous lithium bromide. *International Journal of Refrigeration*, 18(7):486-494.

Kostin, Z. A. and V. G. Gorshkov. 1990. Experimental investigation of the processes occurring in a model of the absorbing apparatus of a Lithium-Bromide refrigerating machine with fixed and vibrating tubes.

Kulankara, S. and K. E. Herold. 2002. Surface tension of aqueous lithium bromide with heat/mass transfer enhancement additives: the effect of additive vapor transport. *International Journal of Refrigeration*, 25(3):383-389.

Kyung, I., K. E. Herold and Y. T. Kang. 2007. Model for absorption of water vapor into aqueous LiBr flowing over a horizontal smooth tube. *International Journal of Refrigeration*, 30(4):591-600.

Lee, S., L. K. Bohra, S. Garimella and A. K. Nagavarapu. 2012. Measurement of absorption rates in horizontal-tube falling-film ammonia-water absorbers. *International Journal of Refrigeration*, 35(3):613-632.

Lemlich, R. 1955. Effect of Vibration on Natural Convective Heat Transfer. *Industrial & Engineering Chemistry*, 6(1175-1180.

Lemlich, R. and M. R. Levy. 1961. The effect of vibration on natural convective mass transfer. *AIChE Journal*, 7(2):240-242.

Liu, Y. L., S. M. Xu, W. Han and B. Wang. 2004. Experimental study of falling film absorption in a swaying tube using TFE/NMP as working fluid. *Journal of Dalian University of Technology*, 44(1):65-69.

Melendez, D. M. 2010. Effect of ultrasonic vibration on the mass transfer coefficient in a sieve plate scrubber. Master, Clemson University.

Nosoko, T., A. Miyara and T. Nagata. 2002. Characteristics of falling film flow on completely wetted horizontal tubes and the associated gas absorption. *International Journal of Heat and Mass Transfer*, 45(13):2729-2738.

Papaefthimiou, V. D., I. P. Koronaki, D. C. Karampinos and E. D. Rogdakis. 2012. A novel approach for modelling LiBr-H2O falling film absorption on cooled horizontal bundle of tubes. *International Journal of Refrigeration*, 35(4):1115-1122.

Park, C. W., H. C. Cho and Y. T. Kang. 2004. The effect of heat transfer additive and surface roughness of micro-scale hatched tubes on absorption performance. *International Journal of Refrigeration*, 27(3):264-270.

Rameshkumar, A., M. Udayakumar and R. Saravanan. 2009. Heat transfer studies on a GAXAC (generator-absorber-exchange absorption compression) cooler. *Applied Energy*, 86(10):2056–2064.

Seol, S. S. and S. Y. Lee. 2005. Experimental study of film flow and heat/mass transfer in LiBr–H2O solution flowing over a cooled horizontal tube. *International Communications in Heat and Mass Transfer*, 32(3):445-453.

Sirwan, R., M. A. Alghoul, K. Sopian, Y. Ali and J. Abdulateef. 2013. Evaluation of adding flash tank to solar combined ejector–absorption refrigeration system. *Solar Energy*, 91(-):283-296.

Soto Frances, V. M. and J. M. Pinanzo Ojer. 2004. Multi-factorial study of the absorption process of H2O (vap) by a LiBr (aq) in a horizontal tube bundle using 2-ethyl-1-hexanol as surfactant. *International Journal of Heat and Mass Transfer*, 47(14):3355–3373.

Sultana, P., N. E. Wijeysundera, J. C. Ho and C. Yap. 2007. Modeling of horizontal tube-bundle absorbers of absorption cooling systems. *International Journal of Refrigeration*, 30(4):709-723.

Tierney, M. J. 2007. Options for solar-assisted refrigeration—Trough collectors and double-effect chillers. *Renewable Energy*, 32(2):183-199.

Tsuda, H. and H. Perez-Blanco. 2001. An experimental study of a vibrating screen as means of absorption enhancement. *International Journal of Heat and Mass Transfer*, 44(21):4087-4094.

Yigit, A. 1999. A numerical study of heat and mass transfer in falling film absorber. *International communications in heat and mass transfer*, 26(2):269-278.

Yuan, Z. and K. E. Herold. 2001. Surface tension of pure water and aqueous lithium bromide with 2-ethyl-hexanol. *Applied Thermal Engineering*, 21(8):881-897.

Behfar, A., Z. Shen, J Lau, and Y. Yu, (2014) Heat and mass transfer enhancement potential on falling film absorbers for water-LiBr mixtures via a literature review (RP-1462), *HVAC&R Research*, Volume 20, Issue 5, 570-580

Jayasekara, S., and S. K. Halgamuge, (2013) Mathematical modeling and experimental verification of an absorption chiller including three dimensional temperature and concentration distributions, *Applied Energy*, Volume 106, 232–242

Lansing F. L., Computer modeling of a single-stage lithium bromide/water absorption refrigeration unit, *Deep Space Network Progress Report*, January 1976.

Wang K., Abdelaziz O. Vineyard E. A., Thermophysical Properties of Lithium Bromide + 1, 2-Propanediol Aqueous Solutions— Solubility, Density and Viscosity, *International refrigeration and air conditioning conference*, 2157, July 2012

Appendix

A. Continuous heat & mass transfer and cooling performance results (with 2EH additive)

A.1. 15Hz 0.2mm

Frequency 15(Hz)			50 minutes' vibration	
Amplitude 0.2mm/0.0079inch			Amplitude to thickness ratio (%)	31
Solution flow rate (GPM/m^3/h)	1.32	0.3	Mass transfer enhancement (%)	9
Chilled water inlet temperature (°F/°C)	57.38	14.1	Heat transfer enhancement (%)	9.9
Cooling water inlet (°F/°C)	84.92	29.4	Cooling enhancement (%)	14.5
Evaporating temperature (°F/°C)	51.44	10.8	Mass transfer standard deviation (%)	1.8
Hot water temperature (°F/°C)	197.6	92	Heat transfer standard deviation (%)	3
Absorber pressure (psi/kPa)	0.2842	1.96	T difference standard deviation (%)	2.5

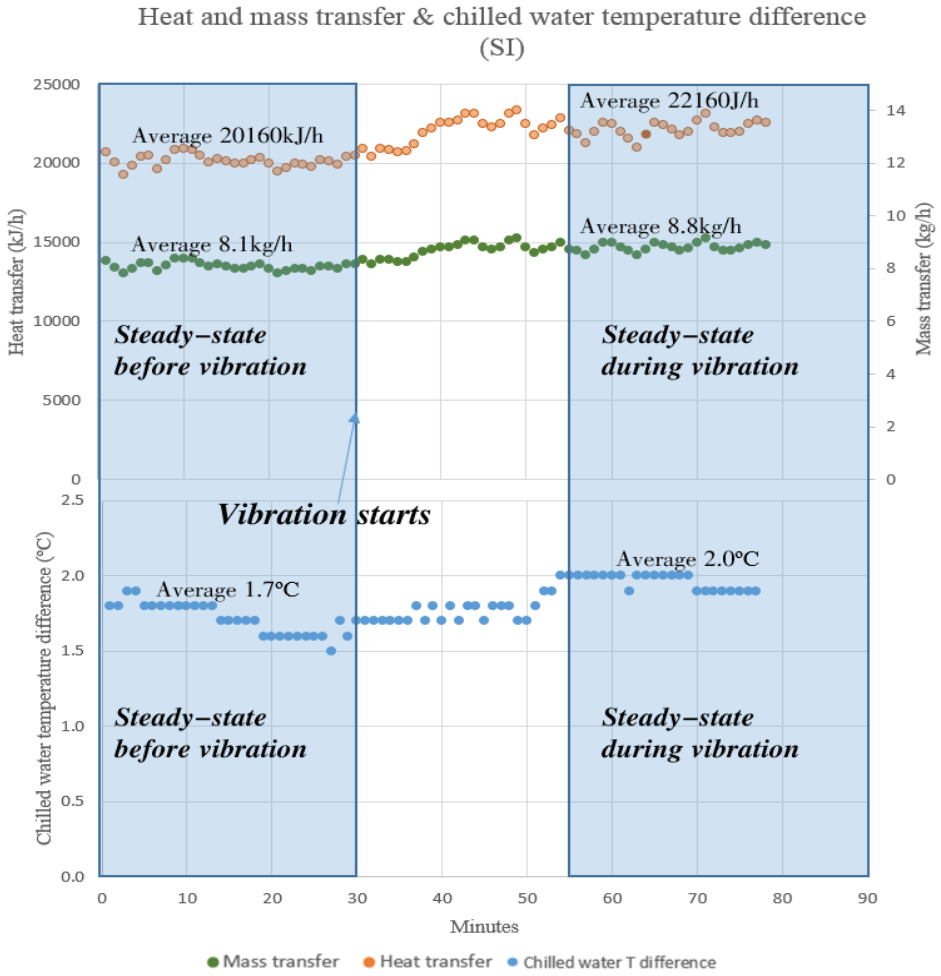

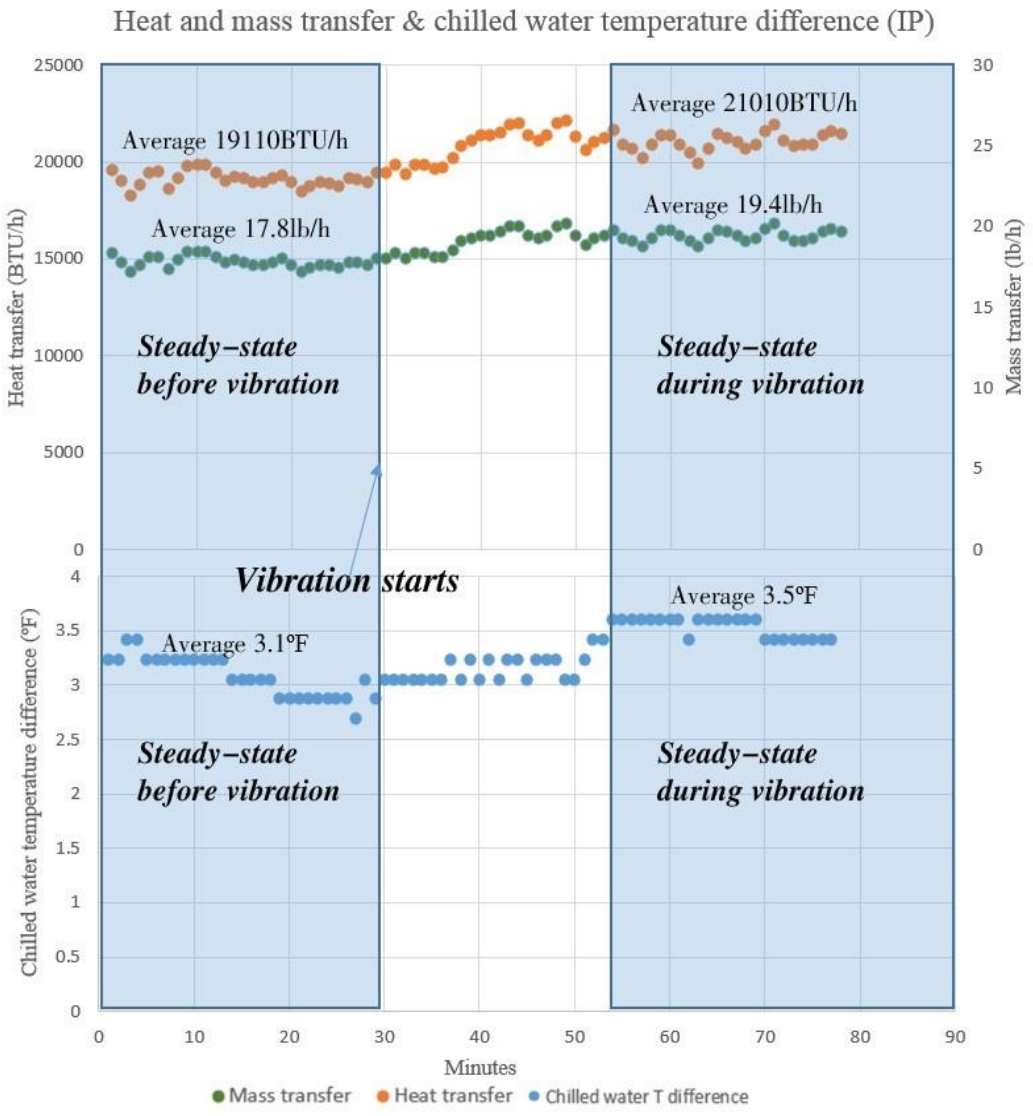
Heat and mass transfer & chilled water temperature difference (IP)
Heat transfer (BTU/h)
Mass transfer (lb/h)
Chilled water temperature difference (°F)
Minutes
Average 19110BTU/h
Average 21010BTU/h
Average 17.8lb/h
Average 19.4lb/h
Steady−state before vibration
Steady−state during vibration
Vibration starts
Average 3.1°F
Average 3.5°F
Steady−state before vibration
Steady−state during vibration
Mass transfer
Heat transfer
Chilled water T difference

A.2. 20Hz 0.2mm

Frequency 20(Hz)			45 minutes' vibration	
Amplitude 0.2mm/0.0079inch			Amplitude to thickness ratio (%)	31
Solution flow rate (GPM/m^3/h)	1.32	0.3	Mass transfer enhancement (%)	22.2
Chilled water inlet temperature (°F/°C)	57.38	14.1	Heat transfer enhancement (%)	22
Cooling water inlet (°F/°C)	84.74	29.3	Cooling enhancement (%)	11.7
Evaporating temperature (°F/°C)	51.08	10.6	Mass transfer standard deviation (%)	1.6
Hot water temperature (°F/°C)	199.4	93	Heat transfer standard deviation (%)	2.5
Absorber pressure (psi/kPa)	0.3132	2.16	T difference standard deviation (%)	3.5

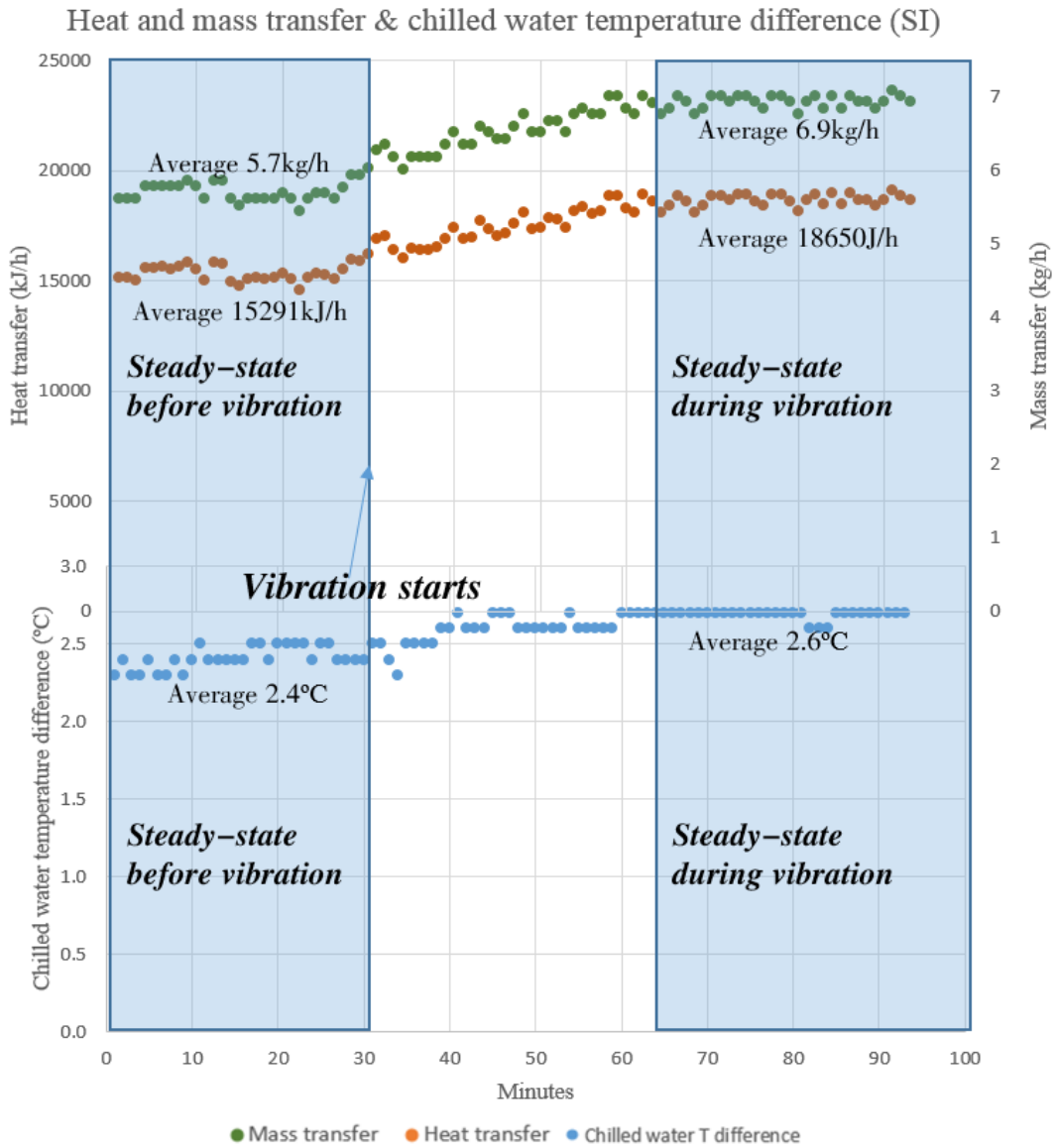

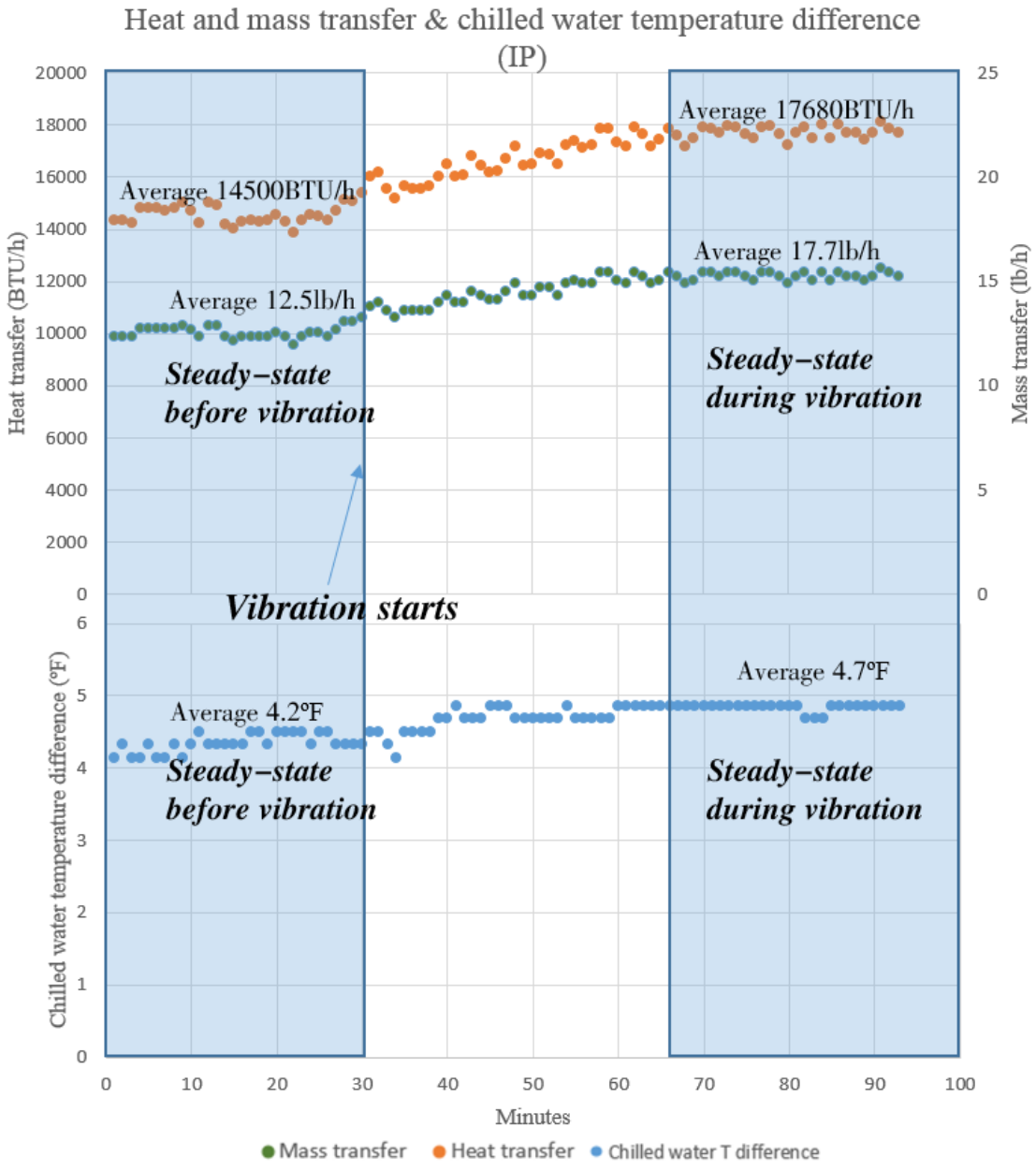
Heat and mass transfer & chilled water temperature difference (IP)
Heat transfer (BTU/h)
Mass transfer (lb/h)
Chilled water temperature difference (°F)
Minutes
Average 14500BTU/h
Average 17680BTU/h
Average 12.5lb/h
Average 17.7lb/h
Steady−state before vibration
Steady−state during vibration
Vibration starts
Average 4.2°F
Average 4.7°F
Steady−state before vibration
Steady−state during vibration
Mass transfer
Heat transfer
Chilled water T difference

A.3. 25Hz 0.2mm

Frequency 25Hz			45 minutes' vibration	
Amplitude 0.2mm/0.0079inch			Amplitude to thickness ratio (%`)	31
Solution flow rate (GPM/m^3/h)	1.32	0.3	Mass transfer enhancement (%)	24.8
Chilled water inlet temperature (°F/°C)	57.38	14.1	Heat transfer enhancement (%)	27.4
Cooling water inlet (°F/°C)	85.1	29.5	Cooling enhancement (%)	13.5
Evaporating temperature (°F/°C)	51.44	10.8	Mass transfer standard deviation (%)	1.8
Hot water temperature (°F/°C)	198.5	92.5	Heat transfer standard deviation (%)	2.4
Absorber pressure (psi/kPa)	0.2929	2.02	T difference standard deviation (%)	2

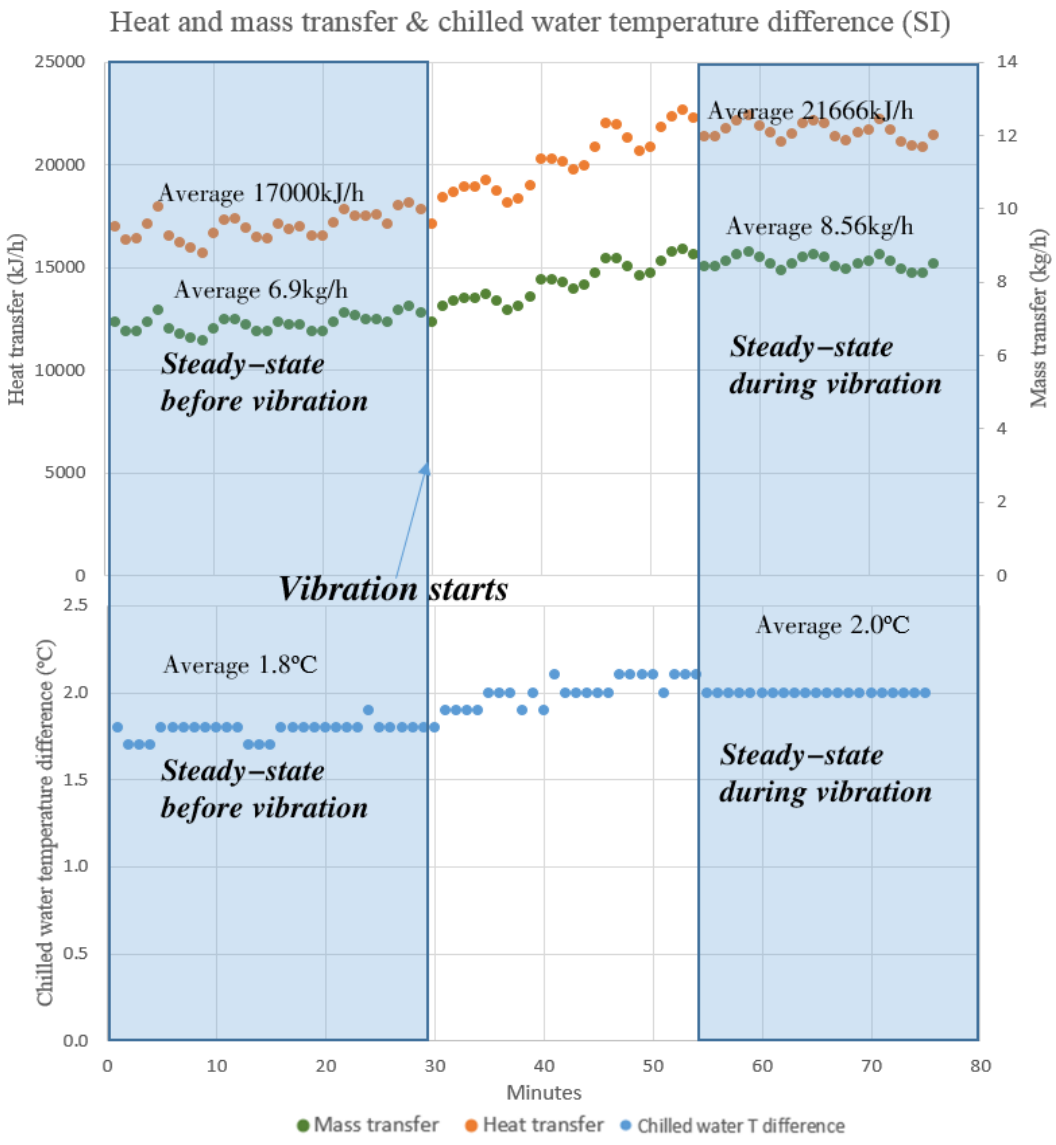

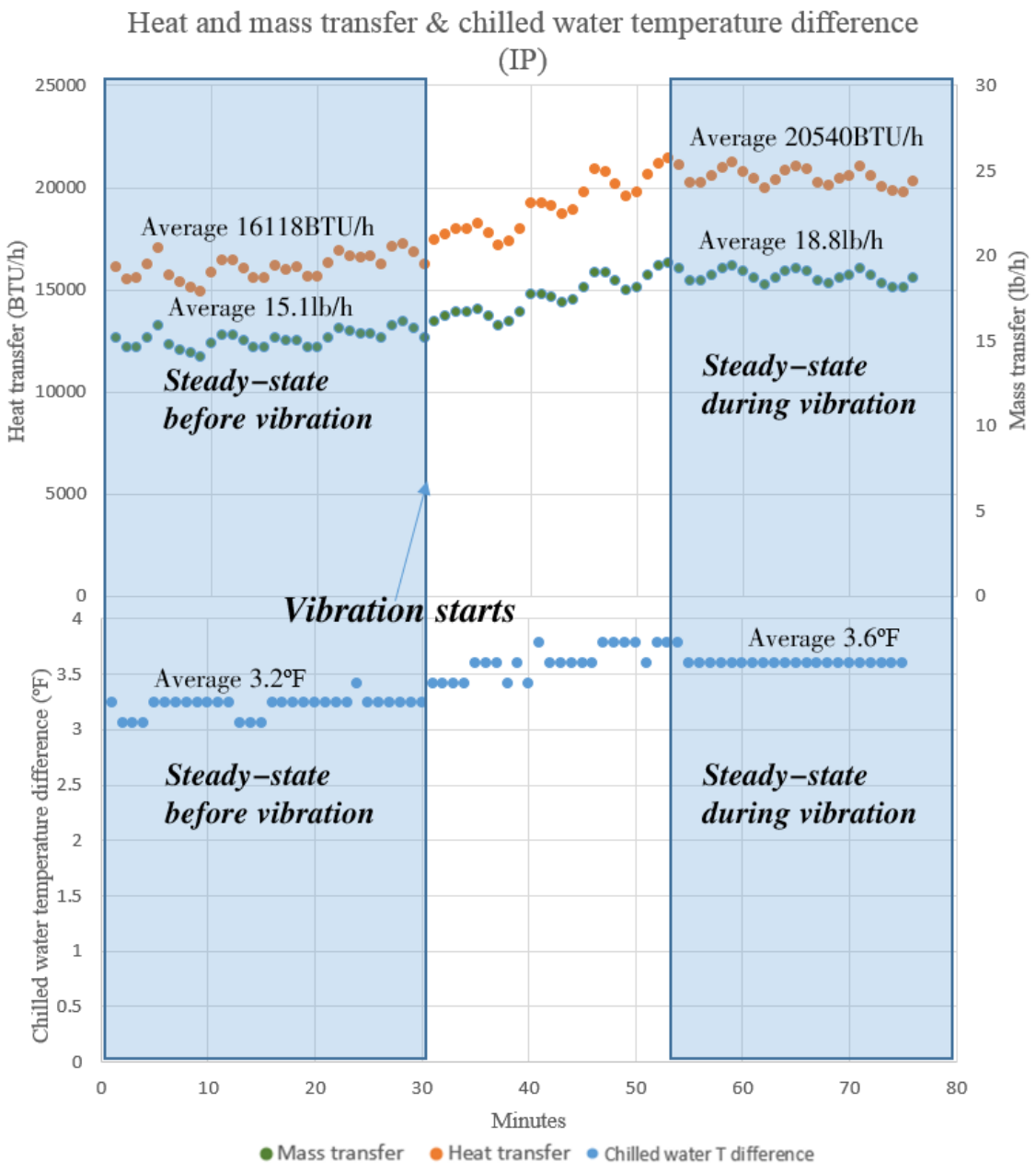
Heat and mass transfer & chilled water temperature difference (IP)
Heat transfer (BTU/h)
Mass transfer (lb/h)
Average 20540BTU/h
Average 16118BTU/h
Average 18.8lb/h
Average 15.1lb/h
Steady−state before vibration
Steady−state during vibration
Vibration starts
Average 3.6°F
Average 3.2°F
Steady−state before vibration
Steady−state during vibration
Chilled water temperature difference (°F)
Minutes
Mass transfer
Heat transfer
Chilled water T difference

A.4. 30Hz 0.2mm

Frequency 30Hz			100 minutes' vibration	
Amplitude 0.2mm/0.0079inch			Amplitude to thickness ratio (%)	31
Solution flow rate (GPM/m3/h)	1.32	0.3	Mass transfer enhancement (%)	19.4
Chilled water inlet temperature (°F/°C)	49.64	9.8	Heat transfer enhancement (%)	21.1
Cooling water inlet (°F/°C)	82.76	28.2	Cooling enhancement (%)	6.7
Evaporating temperature (°F/°C)	46.94	8.3	Mass transfer standard deviation (%)	2.5
Hot water temperature (°F/°C)	202.46	94.7	Heat transfer standard deviation (%)	3.3
Absorber pressure (psi/kPa)	0.2842	1.96	T difference standard deviation (%)	4.1

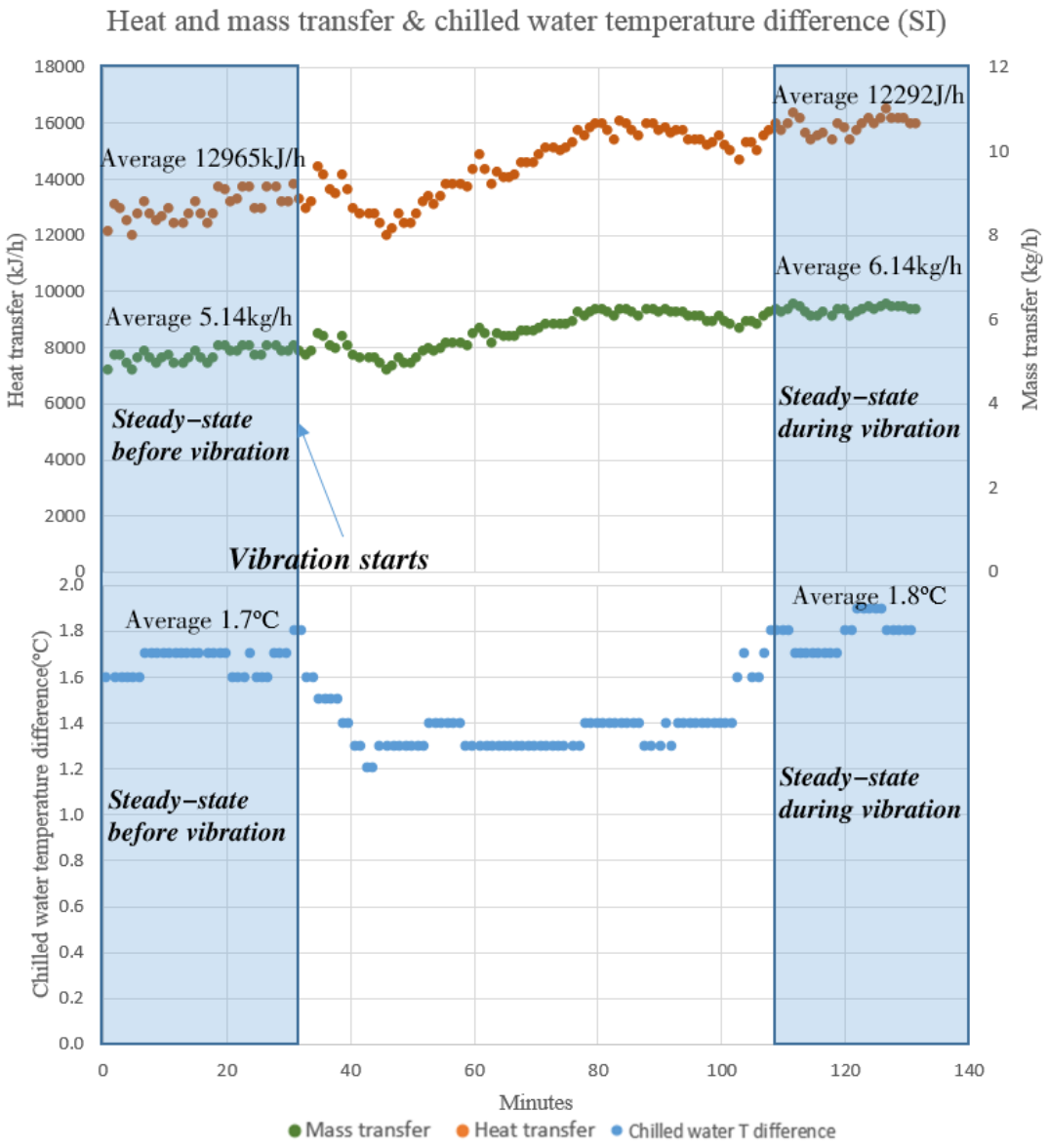

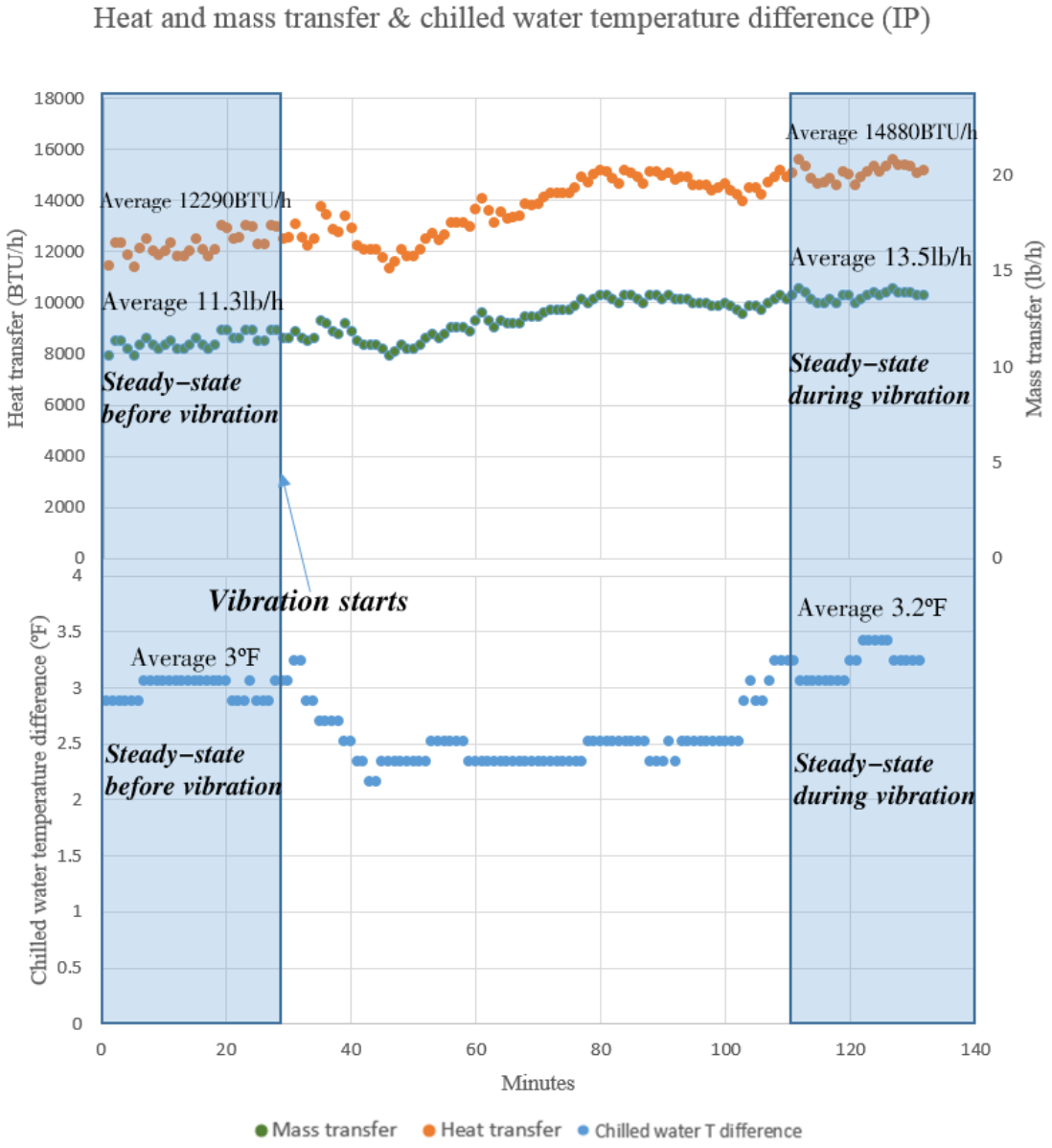
Heat and mass transfer & chilled water temperature difference (IP)
Heat transfer (BTU/h)
Mass transfer (lb/h)
Chilled water temperature difference (°F)
Minutes
Average 12290BTU/h
Average 14880BTU/h
Average 11.3lb/h
Average 13.5lb/h
Steady−state before vibration
Steady−state during vibration
Vibration starts
Average 3°F
Average 3.2°F
Steady−state before vibration
Steady−state during vibration
Mass transfer
Heat transfer
Chilled water T difference

B. Parameters of the key sensors

	Sensor/meter	Description
1	**Platinum Thermal resistance DT-W100--Z/P1/K/S/B/U/02/3/M3-15**	Insertion depth L = 15mm/0.6inch, the cold end 100, the output resistance of the signal, the probe diameter 8mm/0.24inch, threaded M20*1.5, the first waterproof watch
2	**Liquid Turbine Flowmeter LWGY-6/C/05/S/S/N/N**	Media: Lithium bromide, medium temperature 40-80℃/104-176ºF, 30-60℃/86-140oF, DN6, internal thread G1/2,6.3MPA/914psi pressure, live shows + 4-20mA output, precision 0.5, commonly used flow 200kg/h/441lb/h, power supply 24VDC
3	**Liquid Turbine Flowmeter LWGY-25/C/05/S/S/N/N**	Aqueous medium, medium temperature 20-60℃/68-140oF, product temperature of -20-120℃/-4-248oF, range 1-10m^3/h, DN25, internal thread G5/4 or DN25 flange, threaded 6.3MPA/914psi pressure, pressure flange 2.5MPA site display + 4-20mA output, precision 0.5, commonly flow 4200kg/h / 9260lb/h, power supply 24VDC
4	**Liquid Turbine Flowmeter LWGY-25/C/05/W/S/N/N**	Aqueous medium, medium temperature 70-100℃/158-212ºF,0-30℃/32-86ºF, product temperature of -20- 120℃/248ºF, range 0.5-10m^3/h (2.2-4.4GPM), DN25, internal thread G5/4 or DN25 flange, threaded 6.3MPA/914psi pressure, France Portland 2.5MPA pressure, live shows + 4-20mA output, precision 0.5, commonly flow 1550,2000kg/h / 4410lb/h, power supply 24VDC (standard without mating flanges)
5	**Concentration sensor Sensotech Immersion sensor** **40-14**	Standard temperature: 20C to 120C / 68-248ºF optional temperature: to 200ºC/392ºF Standard pressure: 16 bar optional pressure: to 500 bar standard: flange DN50 optional: flange 2" and other Diameter of sensor head: 40mm/1.6inch Diameter of sensor bar: 14mm/0.55inch Immersion length: standard: 92mm/3.6inch Supply 24VDC, 6W Sensor head weight: 6.5kg/14.3lb

C. Summary of long-term experiment results

C.1. Detail information of different solution flow rates enhancement (Without additive)

12/9/2014, Duration: 50 minutes

Frequency 25Hz				
Amplitude 0.2mm/0.0079inch				
Solution flow rate (GPM/m³/h)	**0.88**	**0.2**	**Amplitude to thickness ratio (%)**	**36**
Chilled water inlet temperature (ºF/ºC)	**60.62**	**15.9**	**Mass transfer enhancement (%)**	**38**
Cooling water inlet temperature (ºF/ºC)	**83.3**	**28.5**	**Heat transfer enhancement (%)**	**41.8**
Evaporating temperature (ºF/ºC)	**54.68**	**12.6**	**Cooling enhancement (%)**	**31.4**
Hot water temperature (ºF/ºC)	**204.8**	**96**	**Mass transfer standard deviation (%)**	**2**
Absorber pressure (psi/kPa)	**0.3088**	**2.13**	**Heat transfer standard deviation (%)**	**4.2**

12/10/2014, Duration: 50 minutes

Frequency 25Hz				
Amplitude 0.2mm/0.0079inch				
Solution flow rate (GPM/m³/h)	**1.32**	**0.3**	**Amplitude to thickness ratio (%)**	**31**
Chilled water inlet temperature (ºF/ºC)	**56.66**	**13.7**	**Mass transfer enhancement (%)**	**34.3**
Cooling water inlet temperature (ºF/ºC)	**84.2**	**29**	**Heat transfer enhancement (%)**	**31.7**
Evaporating temperature (ºF/ºC)	**53.96**	**12.2**	**Cooling enhancement (%)**	**53.8**
Hot water temperature (ºF/ºC)	**196.7**	**91.5**	**Mass transfer standard deviation (%)**	**2**
Absorber pressure (psi/kPa)	**0.2987**	**2.06**	**Heat transfer standard deviation (%)**	**3**

1/20/2015, Duration: 60 minutes

Frequency 25Hz				
Amplitude 0.2mm/0.0079inch				
Solution flow rate (GPM/m³/h)	**1.76**	**0.4**	**Amplitude to thickness ratio (%)**	**29**
Chilled water inlet temperature (ºF/ºC)	**59.36**	**15.2**	**Mass transfer enhancement (%)**	**15.6**
Cooling water inlet temperature (ºF/ºC)	**83.66**	**28.7**	**Heat transfer enhancement (%)**	**16.8**
Evaporating temperature (ºF/ºC)	**50.54**	**10.3**	**Cooling enhancement (%)**	**17.4**
Hot water temperature (ºF/ºC)	**202.46**	**94.7**	**Mass transfer standard deviation (%)**	**1.8**
Absorber pressure (psi/kPa)	**0.2842**	**1.96**	**Heat transfer standard deviation (%)**	**2.5**

12/12/2014, Duration: 55 minutes

Frequency 25Hz				
Amplitude 0.2mm/0.0079inch				
Solution flow rate (GPM/m^3/h)	**2.2**	**0.5**	**Amplitude to thickness ratio (%)**	**26**
Chilled water inlet temperature (ºF/ºC)	**60.98**	**16.1**	**Mass transfer enhancement (%)**	**4**
Cooling water inlet temperature (ºF/ºC)	**82.76**	**28.2**	**Heat transfer enhancement (%)**	**4**
Evaporating temperature (ºF/ºC)	**54.86**	**12.7**	**Cooling enhancement (%)**	**1.4**
Hot water temperature (ºF/ºC)	**192.38**	**89.1**	**Mass transfer standard deviation (%)**	**2**
Absorber pressure (psi/kPa)	**0.30885**	**2.13**	**Heat transfer standard deviation (%)**	**3**

C.2. Detail information of different amplitudes enhancement (25Hz) (Without additive)

12/28/2014, Duration: 70 minutes

Frequency 25Hz				
Amplitude 0.1mm/0.0039inch				
Solution flow rate (GPM/m^3/h)	**0.88**	**0.2**	**Amplitude to thickness ratio (%)**	**18**
Chilled water inlet temperature (ºF/ºC)	**64.22**	**17.9**	**Mass transfer enhancement (%)**	**0**
Cooling water inlet temperature (ºF/ºC)	**93.02**	**33.9**	**Heat transfer enhancement (%)**	**0**
Evaporating temperature (ºF/ºC)	**58.1**	**14.5**	**Cooling enhancement (%)**	**12**
Hot water temperature (ºF/ºC)	**203**	**95**	**Mass transfer standard deviation (%)**	**1.5**
Absorber pressure (psi/kPa)	**0.31755**	**2.19**	**Heat transfer standard deviation (%)**	**3**

12/9/2014, Duration: 50 minutes

Frequency 25Hz				
Amplitude 0.2mm/0.0079inch				
Solution flow rate (GPM/m^3/h)	**0.88**	**0.2**	**Amplitude to thickness ratio (%)**	**36**
Chilled water inlet temperature (ºF/ºC)	**60.62**	**15.9**	**Mass transfer enhancement (%)**	**38**
Cooling water inlet temperature (ºF/ºC)	**83.3**	**28.5**	**Heat transfer enhancement (%)**	**41.8**
Evaporating temperature (ºF/ºC)	**54.68**	**12.6**	**Cooling enhancement (%)**	**31.4**
Hot water temperature (ºF/ºC)	**204.8**	**96**	**Mass transfer standard deviation (%)**	**2**
Absorber pressure (psi/kPa)	**0.30885**	**2.13**	**Heat transfer standard deviation (%)**	**4.2**

12/28/2014, Duration: 70 minutes

Frequency 25Hz				
Amplitude 0.3mm/0.0118inch				
Solution flow rate (GPM/m^3/h)	**0.88**	**0.2**	**Amplitude to thickness ratio (%)**	**54**
Chilled water inlet temperature (ºF/ºC)	**62.96**	**17.2**	**Mass transfer enhancement (%)**	**18**
Cooling water inlet temperature (ºF/ºC)	**93.38**	**34.1**	**Heat transfer enhancement (%)**	**17.5**
Evaporating temperature (ºF/ºC)	**56.48**	**13.6**	**Cooling enhancement (%)**	**12.1**
Hot water temperature (ºF/ºC)	**199.4**	**93**	**Mass transfer standard deviation (%)**	**2.3**
Absorber pressure (psi/kPa)	**0.3219**	**2.22**	**Heat transfer standard deviation (%)**	**3**

12/15/2014, Duration: 60 minutes

Frequency 25Hz				
Amplitude 0.4mm/0.0157inch				
Solution flow rate (GPM/m^3/h)	**0.88**	**0.2**	**Amplitude to thickness ratio (%)**	**72**
Chilled water inlet temperature (ºF/ºC)	**59.18**	**15.1**	**Mass transfer enhancement (%)**	**15.8**
Cooling water inlet temperature (ºF/ºC)	**84.2**	**29**	**Heat transfer enhancement (%)**	**11.4**
Evaporating temperature (ºF/ºC)	**52.88**	**11.6**	**Cooling enhancement (%)**	**13.2**
Hot water temperature (ºF/ºC)	**204.8**	**96**	**Mass transfer standard deviation (%)**	**2**
Absorber pressure (psi/kPa)	**0.2987**	**2.06**	**Heat transfer standard deviation (%)**	**4**

C.3. Detail information of different frequencies enhancement (Without additive)

12/23/2014, Duration: 50 minutes

Frequency 15Hz				
Amplitude 0.2mm/0.0079inch				
Solution flow rate (GPM/m^3/h)	1.32	0.3	Amplitude to thickness ratio (%)	31
Chilled water inlet temperature (ºF/ºC)	59.9	15.5	Mass transfer enhancement (%)	4.5
Cooling water inlet temperature(ºF/ºC)	84.2	29	Heat transfer enhancement (%)	4
Evaporating temperature(ºF/ºC)	53.78	12.1	Cooling enhancement (%)	7
Hot water temperature(ºF/ºC)	203	95	Mass transfer standard deviation (%)	2
Absorber pressure (psi/kPa)	0.3074	2.12	Heat transfer standard deviation (%)	3

1/1/2015, Duration: 70 minutes

Frequency 20Hz				
Amplitude 0.2mm/0.0079inch				
Solution flow rate (GPM/m^3/h)	1.32	0.3	Amplitude to thickness ratio (%)	31
Chilled water inlet temperature (ºF/ºC)	59	15	Mass transfer enhancement (%)	10.6
Cooling water inlet temperature (ºF/ºC)	83.84	28.8	Heat transfer enhancement (%)	8.5
Evaporating temperature(ºF/ºC)	56.3	13.5	Cooling enhancement (%)	10.3
Hot water temperature (ºF/ºC)	195.08	90.6	Mass transfer standard deviation (%)	2
Absorber pressure(psi/kPa)	0.306	2.11	Heat transfer standard deviation (%)	3.5

12/10/2014, Duration: 50 minutes

Frequency 25Hz				
Amplitude 0.2mm/0.0079inch				
Solution flow rate (GPM/m^3/h)	1.32	0.3	Amplitude to thickness ratio (%)	31
Chilled water inlet temperature (ºF/ºC)	56.66	13.7	Mass transfer enhancement (%)	34.3
Cooling water inlet temperature (ºF/ºC)	84.2	29	Heat transfer enhancement (%)	31.7
Evaporating temperature(ºF/ºC)	53.96	12.2	Cooling enhancement (%)	53.8
Hot water temperature (ºF/ºC)	196.7	91.5	Mass transfer standard deviation (%)	2
Absorber pressure(psi/kPa)	0.2987	2.06	Heat transfer standard deviation (%)	3

12/21/2014, Duration: 35 minutes

Frequency 30Hz				
Amplitude 0.2mm/0.0079inch				
Solution flow rate (GPM/m^3/h)	1.32	0.3	Amplitude to thickness ratio (%)	74
Chilled water inlet temperature (ºF/ºC)	60.8	16	Mass transfer enhancement (%)	10.7
Cooling water inlet temperature (ºF/ºC)	84.7	29.3	Heat transfer enhancement (%)	8.7
Evaporating temperature(ºF/ºC)	58.1	13	Cooling enhancement (%)	15.7
Hot water temperature (ºF/ºC)	203.8	95.4	Mass transfer standard deviation (%)	3.4
Absorber pressure (psi/kPa)	0.3103	2.14	Heat transfer standard deviation (%)	5

C.4. Detail information of different solution flow rates enhancement (With 2EH additive)

5/7/2015 Duration: 50 minutes

Frequency 25(Hz)				
Amplitude 0.2mm/0.0079inch				
Solution flow rate (GPM/m^3/h)	**0.44**	**0.1**	**Amplitude to thickness ratio (%)**	**45**
Chilled water inlet temperature (ºF/ºC)	**55.04**	**12.8**	**Mass transfer enhancement (%)**	**7.4**
Cooling water inlet temperature (ºF/ºC)	**84.2**	**29**	**Heat transfer enhancement (%)**	**8.7**
Evaporating temperature (ºF/ºC)	**50**	**10**	**Cooling enhancement (%)**	**59**
Hot water temperature (ºF/ºC)	**209.3**	**98.5**	**Mass transfer standard deviation (%)**	**2**
Absorber pressure (psi/kPa)	**0.2871**	**1.98**	**Heat transfer standard deviation (%)**	**3**

4/2/2015 Duration: 50 minutes

Frequency 25(Hz)				
Amplitude 0.2mm/0.0079inch				
Solution flow rate (GPM/m^3/h)	**0.88**	**0.2**	**Amplitude to thickness ratio (%)**	**36**
Chilled water inlet temperature (ºF/ºC)	**56.48**	**13.6**	**Mass transfer enhancement (%)**	**28.7**
Cooling water inlet temperature (ºF/ºC)	**84.02**	**28.9**	**Heat transfer enhancement (%)**	**34**
Evaporating temperature (ºF/ºC)	**51.62**	**10.9**	**Cooling enhancement (%)**	**9.4**
Hot water temperature (ºF/ºC)	**205.7**	**96.5**	**Mass transfer standard deviation (%)**	**3**
Absorber pressure (psi/kPa)	**0.2827**	**1.95**	**Heat transfer standard deviation (%)**	**5**

3/17/2015, Duration: 42 minutes

Frequency 25(Hz)				
Amplitude 0.2mm/0.0079inch				
Solution flow rate (GPM/m^3/h)	**1.32**	**0.3**	**Amplitude to thickness ratio (%)**	**31**
Chilled water inlet temperature (ºF/ºC)	**59.18**	**15.1**	**Mass transfer enhancement (%)**	**21.5**
Cooling water inlet temperature (ºF/ºC)	**84.02**	**28.9**	**Heat transfer enhancement (%)**	**17.8**
Evaporating temperature (ºF/ºC)	**50.9**	**10.5**	**Cooling enhancement (%)**	**5.3**
Hot water temperature (ºF/ºC)	**198.5**	**92.5**	**Mass transfer standard deviation (%)**	**2**
Absorber pressure (psi/kPa)	**0.2871**	**1.98**	**Heat transfer standard deviation (%)**	**4**

5/7/2015, Duration: 60 minutes

Frequency 25(Hz)				
Amplitude 0.2mm/0.0079inch				
Solution flow rate (GPM/m^3/h)	**1.76**	**0.4**	**Amplitude to thickness ratio (%)**	**29**
Chilled water inlet temperature (ºF/ºC)	**51.8**	**11**	**Mass transfer enhancement (%)**	**16.7**
Cooling water inlet temperature (ºF/ºC)	**83.84**	**28.8**	**Heat transfer enhancement (%)**	**19.8**
Evaporating temperature (ºF/ºC)	**45.32**	**7.4**	**Cooling enhancement (%)**	**15.2**
Hot water temperature (ºF/ºC)	**202.64**	**94.8**	**Mass transfer standard deviation (%)**	**1.8**
Absorber pressure (psi/kPa)	**0.2755**	**1.9**	**Heat transfer standard deviation (%)**	**4**

C.5. Detail information of different amplitudes enhancement (With 2EH additive)\

5/14/2015, Duration: 45 minutes

Frequency 25(Hz)				
Amplitude 0.1mm/0.0039inch				
Solution flow rate (GPM/m^3/h)	**0.88**	**0.2**	**Amplitude to thickness ratio (%)**	**18**
Chilled water inlet temperature (ºF/ºC)	**55.4**	**13**	**Mass transfer enhancement (%)**	**16.6**
Cooling water inlet (ºF/ºC)	**82.4**	**28**	**Heat transfer enhancement (%)**	**18.7**
Evaporating temperature (ºF/ºC)	**50**	**10**	**Cooling enhancement (%)**	**9**
Hot water temperature (ºF/ºC)	**197.6**	**92**	**Mass transfer standard deviation (%)**	**2**
Absorber pressure (psi/kPa)	**0.2755**	**1.9**	**Heat transfer standard deviation (%)**	**4**

4/2/2015 Duration: 50 minutes

Frequency 25(Hz)				
Amplitude 0.2mm/0.0079inch				
Solution flow rate (GPM/m^3/h)	**0.88**	**0.2**	**Amplitude to thickness ratio (%)**	**36**
Chilled water inlet temperature (ºF/ºC)	**56.48**	**13.6**	**Mass transfer enhancement (%)**	**28.7**
Cooling water inlet temperature (ºF/ºC)	**84.02**	**28.9**	**Heat transfer enhancement (%)**	**34**
Evaporating temperature (ºF/ºC)	**51.62**	**10.9**	**Cooling enhancement (%)**	**9.4**
Hot water temperature (ºF/ºC)	**205.7**	**96.5**	**Mass transfer standard deviation (%)**	**3**
Absorber pressure (psi/kPa)	**0.2827**	**1.95**	**Heat transfer standard deviation (%)**	**5**

3/28/2015, Duration: 45 minutes

Frequency 25(Hz)				
Amplitude 0.3mm/0.0118inch				
Solution flow rate (GPM/m^3/h)	**0.88**	**0.2**	**Amplitude to thickness ratio (%)**	**54**
Chilled water inlet temperature (ºF/ºC)	**58.28**	**14.6**	**Mass transfer enhancement (%)**	**27.8**
Cooling water inlet temperature (ºF/ºC)	**84.02**	**28.9**	**Heat transfer enhancement (%)**	**29.4**
Evaporating temperature (ºF/ºC)	**52.88**	**11.6**	**Cooling enhancement (%)**	**14.1**
Hot water temperature (ºF/ºC)	**206.78**	**97.1**	**Mass transfer standard deviation (%)**	**3**
Absorber pressure (psi/kPa)	**0.2885**	**1.99**	**Heat transfer standard deviation (%)**	**4**

5/19/2015, Duration: 60 minutes

Frequency 25(Hz)				
Amplitude 0.4mm/0.0157inch				
Solution flow rate (GPM/m^3/h)	**0.88**	**0.2**	**Amplitude to thickness ratio (%)**	**72**
Chilled water inlet temperature (ºF/ºC)	**56.12**	**13.4**	**Mass transfer enhancement (%)**	**12.6**
Cooling water inlet temperature (ºF/ºC)	**81.86**	**27.7**	**Heat transfer enhancement (%)**	**14**
Evaporating temperature (ºF/ºC)	**49.1**	**9.5**	**Cooling enhancement (%)**	**1.9**
Hot water temperature (ºF/ºC)	**201.2**	**94**	**Mass transfer standard deviation (%)**	**2**
Absorber pressure (psi/kPa)	**0.2885**	**1.99**	**Heat transfer standard deviation (%)**	**4**

C.6. Detail information of different frequencies enhancement (With 2EH additive)

4/2/2015, Duration: 50 minutes

Frequency 15(Hz)				
Amplitude 0.2mm/0.0079inch				
Solution flow rate (GPM/m^3/h)	1.32	0.3	Amplitude to thickness ratio (%)	31
Chilled water inlet temperature (ºF/ºC)	57.38	14.1	Mass transfer enhancement (%)	9
Cooling water inlet temperature (ºF/ºC)	84.92	29.4	Heat transfer enhancement (%)	9.9
Evaporating temperature (ºF/ºC)	51.44	10.8	Cooling enhancement (%)	14.5
Hot water temperature (ºF/ºC)	197.6	92	Mass transfer standard deviation (%)	1.8
Absorber pressure (psi/kPa)	0.2842	1.96	Heat transfer standard deviation (%)	3

3/22/2015, Duration: 45 minutes

Frequency 20(Hz)				
Amplitude 0.2mm/0.0079inch				
Solution flow rate (GPM/m^3/h)	1.32	0.3	Amplitude to thickness ratio (%)	31
Chilled water inlet temperature (ºF/ºC)	57.38	14.1	Mass transfer enhancement (%)	22.2
Cooling water inlet temperature (ºF/ºC)	84.74	29.3	Heat transfer enhancement (%)	22
Evaporating temperature (ºF/ºC)	51.08	10.6	Cooling enhancement (%)	11.7
Hot water temperature (ºF/ºC)	199.4	93	Mass transfer standard deviation (%)	1.6
Absorber pressure (psi/kPa)	0.3132	2.16	Heat transfer standard deviation (%)	2.5

4/1/2015, Duration: 45 minutes

Frequency 25Hz				
Amplitude 0.2mm/0.0079inch				
Solution flow rate (GPM/m^3/h)	1.32	0.3	Amplitude to thickness ratio (%)	31
Chilled water inlet temperature (ºF/ºC)	57.38	14.1	Mass transfer enhancement (%)	24.8
Cooling water inlet temperature (ºF/ºC)	85.1	29.5	Heat transfer enhancement (%)	27.4
Evaporating temperature (ºF/ºC)	51.44	10.8	Cooling enhancement (%)	13.5
Hot water temperature (ºF/ºC)	198.5	92.5	Mass transfer standard deviation (%)	1.8
Absorber pressure (psi/kPa)	0.2929	2.02	Heat transfer standard deviation (%)	2.4

4/27/2015, Duration: 100 minutes

Frequency 30Hz				
Amplitude 0.2mm/0.0079inch				
Solution flow rate (GPM/m^3/h)	1.32	0.3	Amplitude to thickness ratio (%)	31
Chilled water inlet temperature (ºF/ºC)	49.64	9.8	Mass transfer enhancement (%)	19.4
Cooling water inlet temperature (ºF/ºC)	82.76	28.2	Heat transfer enhancement (%)	21.1
Evaporating temperature (ºF/ºC)	46.94	8.3	Cooling enhancement (%)	6.7
Hot water temperature (ºF/ºC)	202.46	94.7	Mass transfer standard deviation (%)	2.5
Absorber pressure (psi/kPa)	0.2842	1.96	Heat transfer standard deviation (%)	3.3